NRL Report 6851

The Scattering of a Plane Electromagnetic Wave By a Linear Array of Center-Loaded Cylinders

O. D. Sledge

Radar Analysis Staff
Radar Division

June 6, 1968

NAVAL RESEARCH LABORATORY
Washington, D.C.

45

CONTENTS

ABSTRACT

The scattering properties of a linear array of parallel, center-loaded, cylindrical elements have been investigated with the ultimate objective of obtaining information about the character of the array from its scattered field. To this end, a set of integral equations for the currents induced in the linear array illuminated by an incident plane wave were derived from the equations of Maxwell and the boundary conditions at the surface of the array. Using a zero-order approximation to the form of the axial distribution of the induced currents in the array, a pair of complex current coefficients were calculated numerically for each element of the array using a technique incorporating the set of integral equations. The approximation technique gives reasonable accuracy in the calculation of the //-plane, far-zone, scattered field from the induced currents, provided the electrical half-length of the elements of the array is less than $5\pi/4$ radians.

The scattered field of an eight-element array was calculated for various conditions of impedance loading and illumination of the array.

A significant result of this investigation was the discovery that the //-plane scattered field of a linear array of cylindrical elements illuminated by a plane electromagnetic wave consists of two factors: a reflection factor and an interference factor. The interference factor is simply the complex array factor of the array when excited with a uniform amplitude and an element-to-element phase progression of $2\pi(d/\lambda)\sin\phi_{inc}$ radians, where (d/λ) is the interelement spacing of the array in wavelengths and ϕ_{inc} is the angle of incidence of the illumination. The reflection factor turns out to be the //-plane scattered field in the reflected direction where the interference factor becomes unity.

From the interference factor we determined the positions of the grating lobes and the minima of the //-plane scattering pattern of the array for various plane-wave illuminations.

It was found that the plane of polarization of an array, the number of elements, the interelement spacing, and, possibly, the resonant frequency of the elements can be determined from the //-plane scattering characteristics of the passive linear array of cylindrical elements.

PROBLEM STATUS

This is a final report on one aspect of the problem; work on the problem is continuing.

AUTHORIZATION

NRL Problem R02-44
Project ARPA Order 820

Manuscript submitted December 19, 1967.

THE SCATTERING OF A PLANE ELECTROMAGNETIC WAVE BY A LINEAR ARRAY OF CENTER-LOADED CYLINDERS

INTRODUCTION

The majority of the early theoretical investigations of electromagnetic scattering involved the scattering of a plane electromagnetic wave by a highly conducting, simple geometric object, such as a sphere or cylinder. Extensive references to this early work can be found in King and Wu (1). In recent years a number of papers have appeared in the literature which treated certain simple antennas as scattering devices; in particular, the cylindrical antenna has received considerable attention by Chen and Liepa (2) and others. Chen studied the effect of central loading on the induced current on a thin cylinder illuminated by a plane wave at normal incidence. By suitable variation of the load impedance, Garbacz (3) determined certain antenna parameters, such as impedance and power gain, from measurements of the scattering cross section of a single-port antenna for fixed frequency, polarization, and antenna orientation.

The literature contains extensive treatment of the antenna as a transmitter, that is, as a transducer of current and voltage at a terminal pair to electric and magnetic fields radiating into space. The inverse problem of the receiving antenna, that is, a transducer of incident electric and magnetic fields into current and voltage at a terminal pair, has not received a similar amount of attention. This condition of the literature stems from two facts: first, the mathematical problem involved makes the analytical study of the receiving antenna very difficult except in special instances, and, second, the quantity almost invariably of interest in the receiving case is the power delivered by an incident field to the load connected across the antenna terminals. This quantity can be obtained most conveniently from the transmitting properties of the antenna by reciprocity considerations, without a detailed knowledge of the complicated field and current distributions over the surface of the antenna. If, however, we are interested in the antenna as a scatterer, we are concerned not only with the power delivered to the load but also with the distribution of the power density which the antenna scatters into surrounding space. To find the scattered electromagnetic field, we need detailed information about the currents induced on the conducting surfaces of the antenna which radiate the scattered field.

Very little work on the scattering of an electromagnetic wave by an antenna array has appeared in the literature. To improve our knowledge and understanding of array-scattering behavior, we decided to make a theoretical investigation of the scattering of a plane electromagnetic wave by a simple linear array of N parallel, cylindrical, center-loaded elements.

The approach used to solve the steady-state scattering problem is first to find an approximation to the complex currents induced in the elements of the array by the incident illumination. Once the current distribution, in amplitude and phase, along each element of the array is determined, the far-zone scattered field radiated by these currents is easily calculated from the superposition of the radiation fields of the individual elements of the array.

THEORETICAL SKETCH

Theoretical Model

Consider a plane electromagnetic wave of wavelength λ with its electric vector polarized in the z direction incident in the yz plane (x-y plane) of the linear array of N center-loaded cylinders of infinite conductivity positioned in space as shown in Fig. 1. The electromagnetic wave is incident at an angle ϕ_{inc} to the normal to the plane of the array. The central impedances Z_i are lumped, or without physical dimensions. The cylindrical elements of the array are identical, with the exception of the load impedances, each with a half-length h and a radius a. For the sake of simplicity, we assume the elements of the array to be very thin cylinders with half-lengths larger than 400 times their radius. Also, it is assumed that $2\pi a/\lambda$ is less than 0.0100. In the theoretical model chosen, only the induced currents that flow along the length of cylinders contribute significantly to the far-zone scattered field; consequently, the induced currents maintain a retarded vector potential possessing solely a z component. From the symmetry of the array and the uniformity of the phase and amplitude of the incident electric field along the entire length of each cylinder, it follows that the induced currents and their respective vector potentials possess even symmetry in z.

We use a complex notation with the time-dependence factor $\exp(j\omega t)$ of the incident wave suppressed in the treatment of steady-state scattering. The rationalized mks-coulomb system of units is used throughout the report. All alternating (oscillating) quantities are complex unless otherwise indicated.

Derivation of the System of Integral Equations of the Array Currents

Our ultimate purpose is to calculate the scattered field of the array; to do this calculation we first find an approximation to the current induced in each element of the

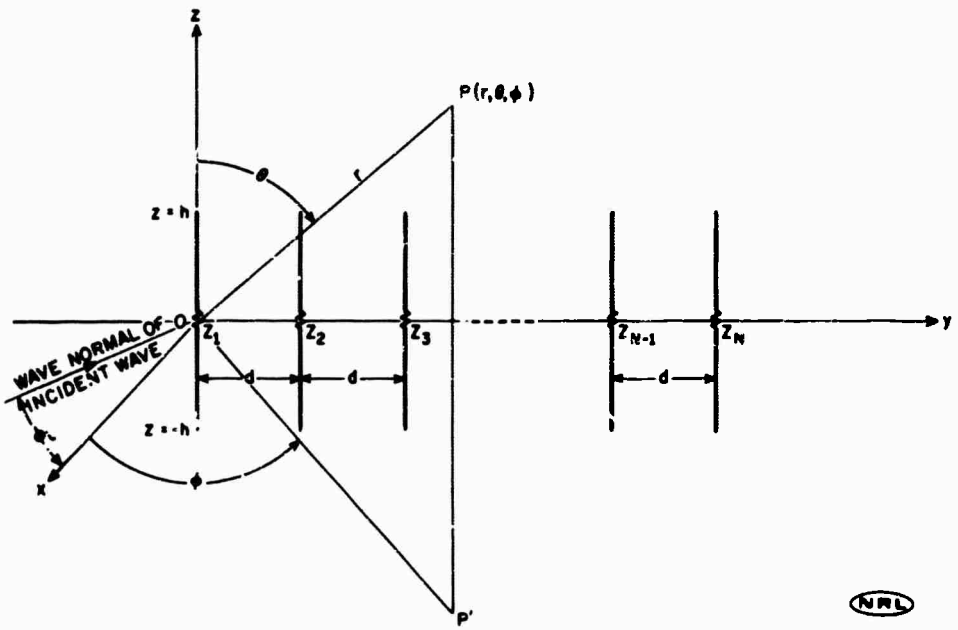

Fig. 1 - The theoretical model

array by the incident illumination. The induced currents must satisfy a system of linear integral equations, which we shall derive in the following pages.

The incident electric field tangential to the surface of the m-th cylinder may be written in the form

$$E^i_{mz} = E_0 \exp(j\psi_m), \tag{1}$$

where E_0 and ψ_m are, respectively, the real amplitude and phase of the incident electric field, each of which is constant along the cylinder. The induced tangential electric field at the surface of the m-th cylinder, maintained by the induced currents and charges on all of the cylinders of the array, is given by

$$E^a_{mz}(z) = -\frac{\partial \Phi_{mz}(z)}{\partial z} - j\omega A_{mz}(z), \tag{2}$$

where A_{mz} is the tangential component of the retarded vector potential on the surface of the m-th cylinder due to all the array currents and Φ_{mz} is the scalar potential on the surface of the m-th element due to the charges on all of the cylindrical surfaces of the array. In the steady state, Φ_{mz} can be eliminated by means of the Lorentz condition (4):

$$\frac{\partial A_{mz}(z)}{\partial z} = -j\omega\epsilon_0\mu_0\Phi_{mz}(z)$$

$$= -j\beta^2\Phi_{mz}(z), \tag{3}$$

where $\beta = 2\pi/\lambda$ is the phase constant of space, ω is the radian frequency of the illumination, ϵ_0 is the permittivity of space, and μ_0 is the permeability of space.

Combining Eqs. (2) and (3), we have

$$E^a_{mz}(z) = -j(\omega/\beta^2)\left[\frac{d^2 A_{mz}(z)}{dz^2} + \beta^2 A_{mz}(z)\right]. \tag{4}$$

The electric field E^g_{mz} across the very small gap of width 2Δ at the center of the m-th cylinder is related to the voltage drop across the center load as follows:

$$\int_{-\Delta}^{\Delta} E^g_{mz}\, dz = Z_m I_m(0), \tag{5}$$

where Z_m is the complex central load impedance and $I_m(0)$ is the current at the center of the m-th element of the array. For our dimensionless load, Δ must approach zero in the limit, and we obtain from Eq. (5)

$$E^g_{mz} = Z_m I_m(0)\,\delta(z), \tag{6}$$

where $\delta(z)$ is the Dirac delta function.

With a perfectly conducting cylinder, the total tangential electric field vanishes at the surface of the cylinder, excluding the infinitesimal region of the central load. This means

$$E^{a}_{mz} + E^{i}_{mz} = 0 \tag{7}$$

along the cylinder, and in the central gap

$$E^{g}_{mz} = E^{a}_{mz} + E^{i}_{mz} = Z_m I_m(0)\,\delta(z). \tag{8}$$

From Eqs. (1), (4), and (8) we obtain the following differential equation for $A_{mz}(z)$ valid over the entire length of the m-th cylinder:

$$\frac{d^2 A_{mz}(z)}{dz^2} + \beta^2 A_{mz}(z) = j(\beta^2/\omega)\,[Z_m I_m(0)\,\delta(z) - E_0 \exp(j\theta_m)]. \tag{9}$$

The general solution of the inhomogenous differential equation (9) consists of the complementary function and a particular integral. The complementary function is given by

$$[A_{mz}(z)]_c = (-j\mathcal{C})(C_1 \cos \beta z + C_2 \sin \beta z), \tag{10}$$

where $\mathcal{C} = 1/(\mu_0 \epsilon_0)^{1/2}$ is the velocity of propagation of electromagnetic waves in free space and C_1 and C_2 are constants of integration. The constant C_2 is zero, since $A_{mz}(z)$ possesses even symmetry in z in our theoretical model. A particular integral can be written as follows:

$$[A_{mz}(z)]_p = (-j/\mathcal{C})\,[(E_0/\beta)(1 - \cos \beta z) \exp(j\theta_m) - (Z_m I_m(0)/2) \sin \beta z], \quad \text{for } 0 \le z \le h, \tag{11a}$$

and

$$[A_{mz}(z)]_p = (-j/\mathcal{C})\,[(E_0/\beta)(1 - \cos \beta z) \exp(j\theta_m) + (Z_m I_m(0)/2) \sin \beta z], \quad \text{for } -h \le z \le 0. \tag{11b}$$

Equations (11) satisfy the differential equation (9) for $-h \le z \le h$. In order for Eqs. (11) to satisfy Eq. (9) at the infinitesimal gap in the center of the m-th cylinder, it is necessary that dA_{mz}/dz possess a jump at $z = 0$ of a magnitude $j\beta^2 Z_m I_m(0)\,\omega$ which in turn assures that d^2A_{mz}/dz^2 contains a delta function of the correct magnitude to balance the impulsive term appearing in the right-hand member of Eq. (9). In shorthand form, the general solution of the differential equation (9) is given by:

$$A_{mz}(z) = (-j/\mathcal{C})\,[C_1 \cos \beta z + (E_0/\beta)(1 - \cos \beta z) \exp(j\theta_m) - (Z_m I_m(0)/2) \sin \beta |z|], \text{ for } -h \le z \le h. \tag{12}$$

Setting $z = \pm h$ in Eq. (12) yields the following expression for C_1:

$$C_1 = \sec \beta h \left\{ (j\mathcal{C}/2)\,[A_{mz}(h) + A_{mz}(-h)] - (E_0/\beta)(1 - \cos \beta h) \exp(j\theta_m) + (Z_m I_m(0)/2) \sin \beta h \right\}. \tag{13}$$

Since $A_{mz}(z)$ is an even function, the expression for C_1 becomes

$$C_1 = \sec \beta h \left\{ j\mathcal{C} A_{mz}(h) - (E_0/\beta)(1 - \cos \beta h) \exp(j\theta_m) + [Z_m I_m(0)/2] \sin \beta h \right\}. \tag{14}$$

From Eqs. (14) and (12) we obtain the following equation:

$$A_{mz}(z) - A_{mz}(h) = (-j/\mathcal{C}) \sec \beta h \left\{ [Z_m I_m(0)/2] \sin \beta(h - |z|) + [j\mathcal{C} A_{mz}(h) - (E_0/\beta) \exp(j\theta_m)] (\cos \beta z - \cos \beta h) \right\}. \tag{15}$$

From its definition, the z component of the retarded vector potential just outside the surface of the m-th cylinder at a distance z from the center of the cylinder is given approximately by the expression

$$A_{mz}(z) \approx (\mu_0/4\pi) \sum_{i=1}^{N} \int_{-h}^{h} I_i(\beta z') K_{mi}(z, z')\, dz' \tag{16}$$

where

$$K_{mi}(z, z') = \frac{\exp\left\{-j\beta[(z-z')^2 + (m-i)^2 d^2]^{1/2}\right\}}{[(z-z')^2 + (m-i)^2 d^2]^{1/2}}, \quad \text{for } m \neq i$$

and

$$K_{mi}(z, z') = \frac{\exp\left\{-j\beta[(z-z')^2 + a^2]^{1/2}\right\}}{[(z-z')^2 + a^2]^{1/2}}, \quad \text{for } m = i,$$

in which d is the center-to-center spacing of the cylindrical elements of the array.

Equation (16) is an accurate representation of the vector potential, except at points very near the ends or the center load of the element. By substituting Eq. (16) into Eq. (15) and letting m assume all integral values from 1 to N, we obtain the following system of linear integral equations for the array of N center-loaded cylinders:

$$\sum_{i=1}^{N} \int_{-h}^{h} I_i(\beta z') [K_{mi}(z, z') - K_{mi}(h, z')]\, dz' = -j \frac{4\pi}{R_0} \sec \beta h \left\{(Z_m I_m(0)/2) \sin \beta(h - |z|) + [jCA_{mz}(h) - (E_0/\beta) \exp(j\beta_m)] (\cos \beta z - \cos \beta h)\right\}, \quad m = 1, 2, 3, \ldots, N, \tag{17}$$

where $R_0 = (\mu_0/\epsilon_0)^{1/2} = 120\pi$ is the characteristic resistance of space.

Approximation Technique

The solution of the system of integral equations of the array to obtain the induced currents in the cylindrical elements is indeed a formidable task and will not be attempted here. Instead, we shall assume the induced currents can be represented by the zero-order approximation

$$I_i(\beta z) = C_i (\cos \beta z - \cos \beta h) + \mathcal{B}_i \sin \beta(h - |z|), \tag{18}$$

where C_i and $\mathcal{B}_i$ are undetermined complex current coefficients. Note that Eq. (18) satisfies the end conditions that I_i vanish at $z = \pm h$, independent of finite C_i and $\mathcal{B}_i$. King (5) suggests that Eq. (18) is an adequate approximation for use in the calculation of the far-zone radiation field of an array of thin cylinders of electrical half-length βh less than $5\pi/4$. The scattered or reradiated field is relatively insensitive to small errors in the current distribution on the array. The current coefficients C_i and $\mathcal{B}_i$ can be determined from the set of integral equations and, thus, take into account the mutual coupling or interaction between the elements of the array.

Using Eq. (18) in Eq. (17), the system of integral equations of the array becomes

$$\sum_{i=1}^{N}\left\{\mathfrak{A}_i\left[U_{mi}^{c}(z)\cos\beta h - M_{mi}(h)\right]F_c(z) + \mathfrak{B}_i\left[U_{mi}^{s}(z)\,F_s(z)\cos\beta h - L_{mi}(h)\,F_c(z)\right]\right\}$$

$$= -j(Z_m/60)\left[\mathfrak{A}_m(1-\cos\beta h) + \mathfrak{B}_m\sin\beta h\right]F_s(z) + j(E_0/30\beta)(\cos\theta_m + j\sin\theta_m)F_c(z),\quad m=1,2,3,\ldots,N, \tag{19}$$

where

$$F_c(z) = \cos\beta z - \cos\beta h,$$

$$F_s(z) = \sin\beta(h-|z|),$$

$$M_{mi}(z) - M_{mi}(h) = U_{mi}^{c}(z)\,F_c(z),$$

$$L_{mi}(z) - L_{mi}(h) = U_{mi}^{s}(z)\,F_s(z),$$

$$M_{mi}(z) = \int_{-h}^{h}(\cos\beta z' - \cos\beta h)\,K_{mi}(z,z')\,dz',$$

$$L_{mi}(z) = \int_{-h}^{h}\sin\beta(h-|z'|)\,K_{mi}(z,z')\,dz'.$$

We desire to determine the complex constants $\mathfrak{A}_i$ and $\mathfrak{B}_i$ from Eq. (19) in such a manner as to cause our zero-order approximation to the induced currents to hold fairly well along the entire length of the elements of the array. In what follows we employ a technique similar to that of Chen and Liepa (2) in the determination of the current coefficients $\mathfrak{A}_i$ and $\mathfrak{B}_i$.

For a given value of βh, the real part of the dominant term ($i=m$) of the sums in Eq. (19) involving $U_{mi}^{c}(z)$ and $U_{mi}^{s}(z)$ varies with z in a manner like $F_c(z)$ and $F_s(z)$, respectively, except near the center and the ends of the elements. Thus, to achieve our objective, it seems reasonable to divide Eq. (19) into the following two sets of equations:

$$\sum_{i=1}^{N}\left\{\mathfrak{A}_i\left[U_{mi}^{c}(z_c)\cos\beta h - M_{mi}(h)\right] - \mathfrak{B}_i L_{mi}(h)\right\} = j(E_0/30\beta)(\cos\theta_m + j\sin\theta_m),\quad m=1,2,\ldots,N, \tag{20}$$

and

$$\sum_{i=1}^{N}\mathfrak{B}_i U_{mi}^{s}(z_s)\cos\beta h = -j(Z_m/60)\left[\mathfrak{A}_m(1-\cos\beta h) + \mathfrak{B}_m\sin\beta h\right],\quad m=1,2,\ldots,N. \tag{21}$$

where z_c and z_s are reference values in z. Equations (20) and (21) are formed by respectively equating the coefficients of $F_c(z)$ and $F_s(z)$ on opposite sides of Eq. (19). For a given angle of incidence and value of βh, the current coefficients $\mathfrak{A}_i$ and $\mathfrak{B}_i$ are determined from Eqs. (20) and (21) considered as a single set of simultaneous linear equations. For best accuracy in the determination of the constants $\mathfrak{A}_i$ and $\mathfrak{B}_i$, we choose z_c and z_s such that the current distribution functions $F_c(z_c)$ and $F_s(z_s)$ remain as large as possible over the range of interest in βh. The reference values z_c and z_s are chosen as follows:

$$z_c = z_s = 0, \quad \text{for } 0 < \beta h < \pi/2,$$

and

$$z_c = 0 \text{ and } z_s = h - \lambda/4, \quad \text{for } \pi/2 < \beta h < 2\pi.$$

When the elements of the array are an odd multiple of half-waves in length, the expression for the element currents takes the simple form.

$$I_i(\beta z) = D_i \cos \beta z. \tag{22}$$

The complex constants D_i are determined from Eq. (19), which becomes, under this condition,

$$-\sum_{i=1}^{N} D_i \Psi_{mi}(h) = (-jZ_m/60) D_m \sin(k\pi/2) + j(E_0/30\beta)(\cos\theta_m + j\sin\theta_m), \quad m = 1, 2, \ldots, N, \tag{23}$$

where k is the odd number of half-wavelengths in the element length. Note that Eqs. (20) and (21) and the preceding discussion about the reference values of z do not apply to this special case.

In the absence of experimental or theoretical information from independent sources on the currents induced in an array of linear elements illuminated by a plane wave, it was necessary to test the approximation technique used in this report to calculate the induced currents in the array. The array currents found by this technique do not satisfy the set of integral equations of the array; however, the approximate currents can be checked in a semiquantitative manner. To achieve this end, we obtain a measure of how much the approximate currents fail to satisfy the set of integral equations (19) of the array. The method of evaluation of the approximate technique and the results obtained for several values of the electrical half-length of the elements are presented in Appendix A. From the work of Appendix A, it was concluded that the approximate technique used in arriving at the induced currents gives reasonable accuracy in the calculation of the scattered field of the currents, provided the electrical half-length of the array elements does not exceed $5\pi/4$.

Also, it is found from numerous calculations that the approximate solution to the array-scattering problem presented in this report satisfies the reciprocity theorem of electromagnetic fields to a high degree of accuracy.

The Far-Zone Scattered Field of the Array

We shall now proceed to the development of an expression for the far-zone scattered field of the array. At the observation point P of Fig. 1, which is at a distance from the array larger than 1000 times the largest dimension of the array, the z component of the far-zone retarded vector potential of the current in the i-th element of the array is given approximately by the expression

$$A_{iz} = \frac{\mu_0 \exp(-j\beta r)}{4\pi r} \int_{-h}^{h} I_i(\beta z') \exp[j\beta(z'\cos\theta + y_i' \sin\theta \sin\phi)]\, dz'. \tag{24}$$

The coordinates r, θ, and ϕ locate the observation point, and z' and $y_i' = (i-1)d$ are the array coordinates. By virtue of the linearity of our physical system, it follows that the vector potential of the array at P is simply the vector sum of vector potentials at the observation point of the individual element currents of the array. Therefore, the vector potential of the array at P is given by

$$A_z = \frac{\mu_0 \exp(-j\beta r)}{4\pi r} \sum_{i=1}^{N} \exp[j(i-1)\beta d \sin\theta \sin\phi] \int_{-h}^{h} I_i(\beta z') \exp(j\beta z' \cos\theta)\, dz' . \tag{25}$$

In the direction (θ, ϕ), the far-zone scattered electric field of the array is related to the vector potential by the expression

$$E_\theta^s = j\beta\mathcal{C} A_z \sin\theta . \tag{26}$$

Putting Eq. (25) in Eq. (26), and using the fact that the element current is an even function of $\beta z'$, we obtain the final form of the expression for the steady-state scattered electric field, namely,

$$E_\theta^s = j \frac{60}{r} \sin\theta \exp(-j\beta r) \sum_{i=1}^{N} \left[\int_0^{\beta h} I_i(u) \cos(u\cos\theta)\, du \right] \exp[j(i-1)\beta d \sin\theta \sin\phi] , \tag{27}$$

where $u = \beta z'$.

In the calculation of the scattered field, it is convenient to make the results independent of the distance from the center of the first element of the array to the point of observation. To achieve this condition, we multiply Eq. (27) by the reciprocal of the quantity $(60/r) \exp(-j\beta r)$ to obtain

$$(E_\theta^s)_n = j \sin\theta \sum_{i=1}^{N} \left[\int_0^{\beta h} I_i(u) \cos(u\cos\theta)\, du \right] \exp[j(i-1)\beta d \sin\theta \sin\phi] . \tag{28}$$

which is defined as the normalized scattered electric field.

The effective scattering coefficient of the i-th element of the array is defined as

$$G_i \exp(j\gamma_i) = \int_0^{\beta h} I_i(u) \cos(u\cos\theta)\, du , \tag{29}$$

where G_i and γ_i are, respectively, the real amplitude and phase of the scattering coefficient. Introducing G_i and γ_i, in Eq. (28), we obtain

$$(E_\theta^s)_n = j \sin\theta \sum_{i=1}^{N} G_i \exp[j(i-1)\beta d \sin\theta \sin\phi + j\gamma_i] \tag{30}$$

It should be understood that both G_i and γ_i are functions of βh, (d/h), the load impedances, and the angle of incidence of the illumination.

Under most conditions of H-plane scattering, it is found from our calculations (Appendix B) that the values of G_i change only a small percentage across the array, and the values of γ_i change approximately linearly across the array. That is, γ_i can be expressed in the form

$$\gamma_i = \gamma_1 - (i-1)\beta d \sin\phi_{inc} , \tag{31}$$

where ϕ_{inc} is the angle of incidence of the illumination and γ_1 is the phase of the scattering coefficient of the first element for non-normal incident illumination or the average phase of the scattering coefficients of the elements of the array in the case of normal incidence. If in Eq. (30) we replace G_i by G_{av}, its average value taken over the array, and

γ_i by the expression given by Eq. (31), Eq. (30) becomes a finite geometric series which can be summed to yield the following approximate formula for the normalized, h plane, scattered field:

$$\left(E_\theta^s\right)_n = G_{av}\left[\frac{\sin\left(N\psi/2\right)}{\sin\left(\psi/2\right)}\right]\exp\left[j\left(\gamma_1 + \frac{\pi}{2} + (N-1)\psi/2\right)\right], \tag{32}$$

where $\psi = \beta d(\sin\phi + \sin\phi_{inc})$.

From extensive calculations we found that Eq. (32) agrees well in both amplitude and phase with Eq. (30), except near the nulls of the function $\sin(N\psi/2)\sin(\psi/2)$ and regions in βh where the array exhibits resonance phenomena. Over the area covered by this investigation, we find that Eq. (32) is quite helpful in the exploration of the general character of the scattered field. Equation (32) is particularly useful and fairly accurate in the determination of the angular positions of the major or grating lobes and the minima of the scattered radiation pattern of the array.

The Positions of the Grating Lobes and the Minima of the //-Plane Scattering Pattern of the Array

It is easily demonstrated from Eq. (32), for an array with fixed physical dimensions and load impedances, illuminated by a plane wave of a given wavelength and angle of incidence, that the major, or grating, lobes of the //-plane scattering pattern are centered approximately at the values of ϕ which satisfy the relation

$$\psi/2 = \pm n\pi$$

or

$$\sin\phi = \pm(2n\pi/\beta d) - \sin\phi_{inc}. \tag{33a}$$

where $n = 0, 1, 2, 3, \ldots$ is the order of the grating lobe. According to Eq. (33a), the zero-order grating lobe is located at the specular observation angle $\phi = -\phi_{inc}$, independent of the electrical interelement spacing βd. The back-scattered grating lobes are centered at $\phi = \phi_{inc}$ by definition. Setting $\phi = \phi_{inc}$ in Eq. (33a), we obtain the condition for the occurrence of a back-scattered grating lobe, namely,

$$\sin\phi_{inc} = \pm n\pi/\beta d. \tag{33b}$$

Table 1 shows the angles of incidence where back-scattered grating lobes occur for various interelement spacings in wavelengths.

Table 1
The Angles of Incidence which Yield Back-Scattered Grating Lobes

d/λ	Angles of Incidence (degrees) n						
	0	1	2	3	4	5	6
1/2	0	90	-	-	-	-	-
1.0	0	30	90	-	-	-	-
3/2	0	19.5	41.8	90	-	-	-
2.0	0	14.5	30	48.6	90	-	-
5/2	0	11.5	23.6	36.9	53.1	90	-
3.0	0	9.6	19.5	30.0	41.8	56.4	90

Also, from Eq. (32) it is observed that the position of the minima of the H-plane scattering pattern are approximately determined by the condition

$$N\psi/2 = \pm k\pi, \quad k = 1, 2, 3, \ldots,$$

or

$$\sin \phi = \pm(2k\pi/N\beta d) - \sin \phi_{inc}. \tag{34}$$

provided $(\psi/2)$ is not zero or an integral multiple of π.

THE RESULTS OF A THEORETICAL STUDY OF THE SCATTERED FIELD OF AN ARRAY

The Model Used in the Investigation

The model used in the investigation is shown in Fig. 1. The model involves an eight-element linear array with uniform load impedances and an interelement spacing equal to the element length. The physical dimensions of the array are considered fixed, while the electrical half-length of the elements βh changes linearly with the frequency of the incident electromagnetic wave. The phase of the incident field at the m-th element of the array is given by

$$\theta_m = (m-1)\beta d \sin \phi_{inc}. \tag{35}$$

The zero-phase reference in all the work to follow is the phase of the incident field at the first element of the array. In our scattering calculations, the ratio of the radius to the length of the elements is fixed at 0.001, and we keep $E_0 h = 30$ to determine the strength of the incident illumination. The numerical investigation of the scattered E field is limited in this report to the H plane of the array.

The Results of the Investigation of Array Scattering

A Typical Set of Array Current Distributions — As an example of the currents induced in the array, we present Fig. 2, which shows the distribution of the in-phase and quadrature components of the axial currents induced in the various elements of the model array of full-wave dipoles with central nonreactive load impedances of 72 ohms by a plane wave incident at -20 degrees. It is evident that both amplitude and phase distribution information is available from these graphs.

An Example of a Polar Scattering Pattern of the Array — Figure 3 shows a polar diagram of the amplitude of the scattered electric field E_ϕ^s of an array of eight half-wave elements with a nonreactive load impedance of 72 ohms when illuminated by a plane electromagnetic wave incident at -40 degrees. Note the major scattering lobes in the reflected direction of 40 degrees and in the forward scattering direction. Also, notice the symmetry of the pattern about the line of the element centers. In reality, the scattered energy in the forward direction is slightly less than in the reflected direction, because the induced surface current density on the shadowed half of the cylinders is slightly less than on the illuminated half of the cylinders.*

*Using the classical formulas (see King and Wu (1), Eq. 13.3, page 39) for the surface current density induced on an infinitely long cylinder of infinite conductivity by a plane electromagnetic wave, we find (for $\beta a = 0.01$) that the surface current density at the center of the shadowed half of the cylinder is reduced in amplitude by 6% and shifted in phase by 11 degrees relative to the current density at a point diametrically opposite in the center of the illuminated half of the cylinder.

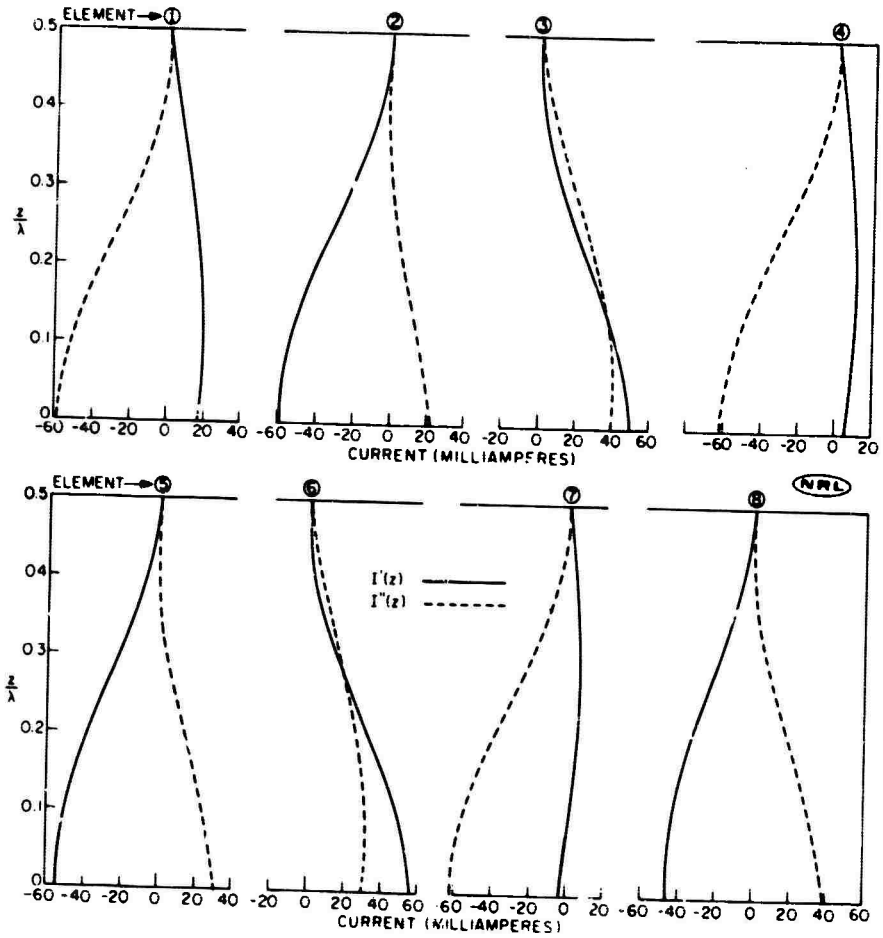

Fig. 2 - The currents induced in the model array of full-wave elements by a plane wave incident at 20 degrees, $I'(z)$ = in-phase component, $I''(z)$ = quadrature component

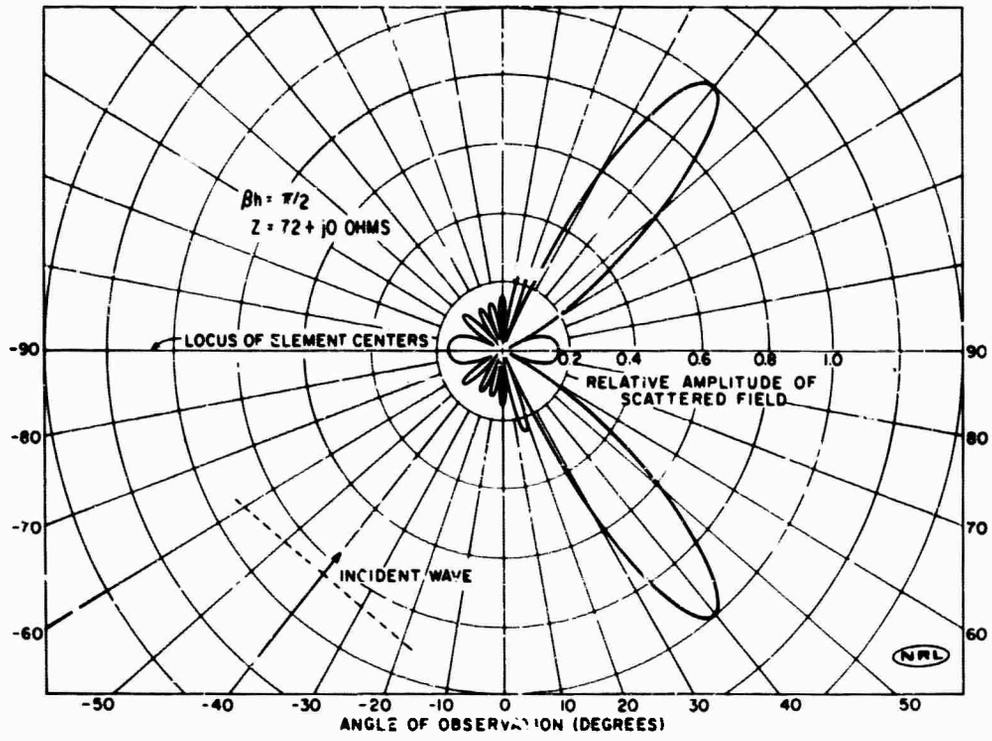

Fig. 3 - A *H*-plane polar scattering diagram of the model array

The Distribution of the Normalized Amplitude of the Scattered Electric Field in $\psi/2$ — In Fig. 4 we present a universal graph of the distribution of the amplitude of the normalized scattered field of the eight-element array under study. The figure shows the reflected lobe centered at $\psi/2 = 0$ and the first-order grating lobes centered at $\psi/2 = \pm\pi$. The solid curve represents the field distribution given by the approximate Eq. (32), while the indicated points are derived from the more accurate formula of Eq. (30). The agreement is quite good considering that the conditions for the points were chosen deliberately to show the greatest possible disagreement between the two formulas. Near the element resonance at $\beta h = 1.57$ and at $\beta h = 3.64$, where the reactance of the load impedance apparently resonates the antenna elements, Eq. (32) is not as good an approximation to Eq. (30) as elsewhere in βh (see Appendix B).

The effect on the scattering pattern of the array resulting from a change in the load impedance is portrayed in Fig. 5. The change in the nonreactive load impedance from 72 ohms to 600 ohms has only a small effect. The points calculated from Eq. (30) again fall closely on the solid curve representing Eq. (32).

It is evident from our study that the normalized solid curve of Fig. 4 holds essentially independent of the load impedance, the angle of incidence, and the frequency of the illumination. Supplemental to the information of Figs. 4 and 5, the actual amplitude of the scattered electric field, obtained from Eq. (30), in the reflected, or specular, direction of observation ($\psi = 0$) under various conditions is presented in Table 2.

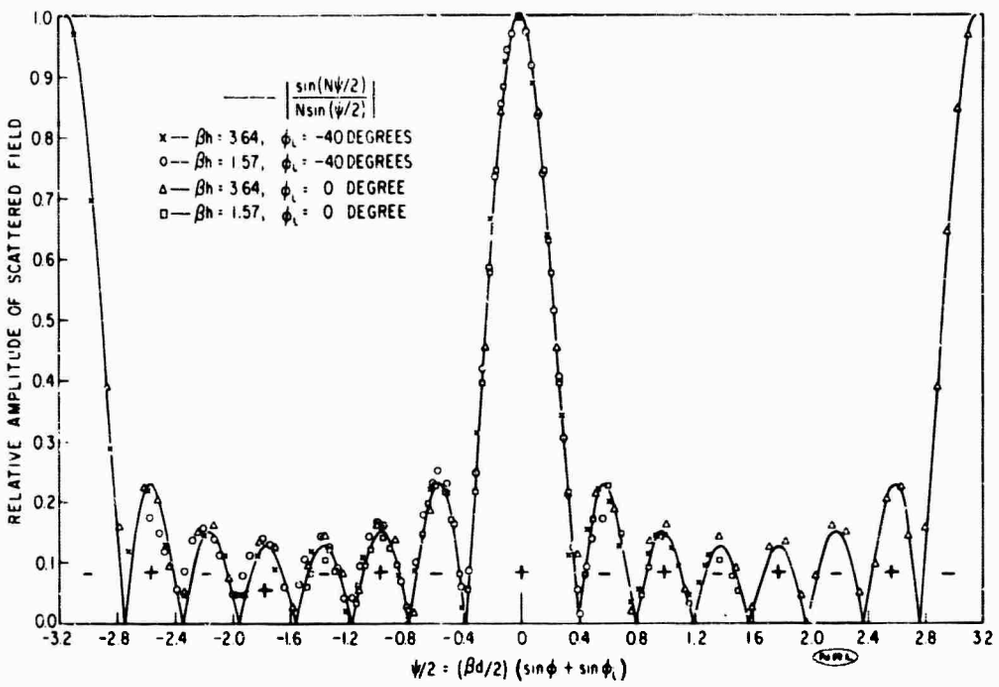

Fig. 4 - A universal *H*-plane scattering pattern of the model array with load impedances: $Z = 72 + j(300\beta\lambda - 740/\beta\lambda)$ ohms

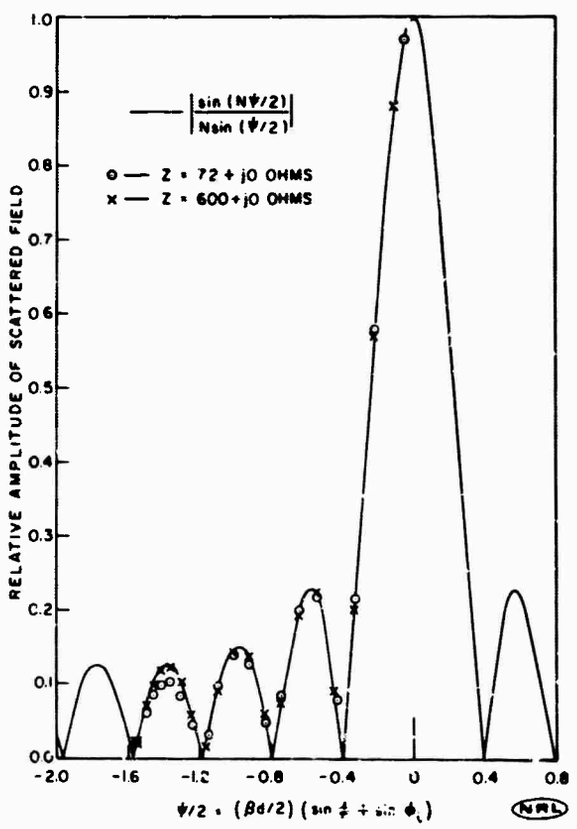

Fig. 5 - The effect of a change in load impedance on the scattering pattern of the model array of half-wave elements illuminated by a plane-wave at normal incidence

Table 2
E_θ^s at the Center of the Reflected Lobe of the Scattering Pattern of the Model Array

Load Impedance Z (ohms)	E_θ^s for Various Values of ϕ_{inc}				
	0°	-10°	-20°	-30°	-40°
$\beta h = \pi/4$					
72 + j0	0.201	0.201	0.202	0.203	0.205
150 + j0	0.196	0.197	0.197	0.198	0.200
300 + j0	0.182	0.182	0.182	0.183	0.184
600 + j0	0.147	0.147	0.147	0.148	0.148
72 + j [300βh - (740/βh)]	0.116	0.117	0.117	0.117	0.118
$\beta h = \pi/2$					
72 + j0	2.390	2.36	2.28	2.15	1.98
150 + j0	1.480	1.47	1.44	1.39	1.32
300 + j0	0.859	0.855	0.845	0.829	0.805
600 + j0	0.466	0.465	0.462	0.457	0.450
72 + j [300βh - (740/βh)]	2.390	2.36	2.28	2.15	1.98
$\beta h = 3\pi/4$					
72 + j0	0.955	0.927	0.799	0.895	0.933
150 + j0	0.925	0.899	0.767	0.830	0.861
300 + j0	0.875	0.853	0.720	0.736	0.755
600 + j0	0.811	0.798	0.675	0.636	0.642
72 + j [300βh - (740/βh)]	0.347	0.345	0.334	0.358	0.364
$\beta h = \pi$					
72 + j0	0.564	0.723	0.782	0.796	0.785
150 + j0	0.568	0.727	0.791	0.806	0.794
300 + j0	0.607	0.784	0.866	0.887	0.870
600 + j0	0.749	1.010	1.15	1.19	1.16
72 + j [300βh - (740/βh)]	0.455	0.472	0.539	0.563	0.543
$\beta h = 5\pi/4$					
72 + j0	0.657	0.570	0.612	0.607	0.583
150 + j0	0.720	0.614	0.670	0.665	0.628
300 + j0	0.877	0.728	0.808	0.802	0.747
600 + j0	1.08	0.875	0.985	0.976	0.902
72 + j [300βh - (740/βh)]	1.73	1.31	1.55	1.53	1.37

The Angular Distribution of the In-Phase and the Phase-Quadrature Components of the Scattered Field — In Fig. 6 we present some examples of the angular distribution of the in-phase and the phase-quadrature components of the H-plane scattered electric field in the half-space on the illuminated side of the linear array. These graphs are obtained from Eq. (30). Note the near symmetry of the field components about the reflected direction of observation for normal incidence and the lack of symmetry exhibited for an angle of incidence of -40 degrees. The effect of changing the load impedance is seen, on comparing Figs. 6a and 6c, to result in merely a change in the level of the scattered field without appreciable change in the angular distribution of its in-phase and phase-quadrature components.

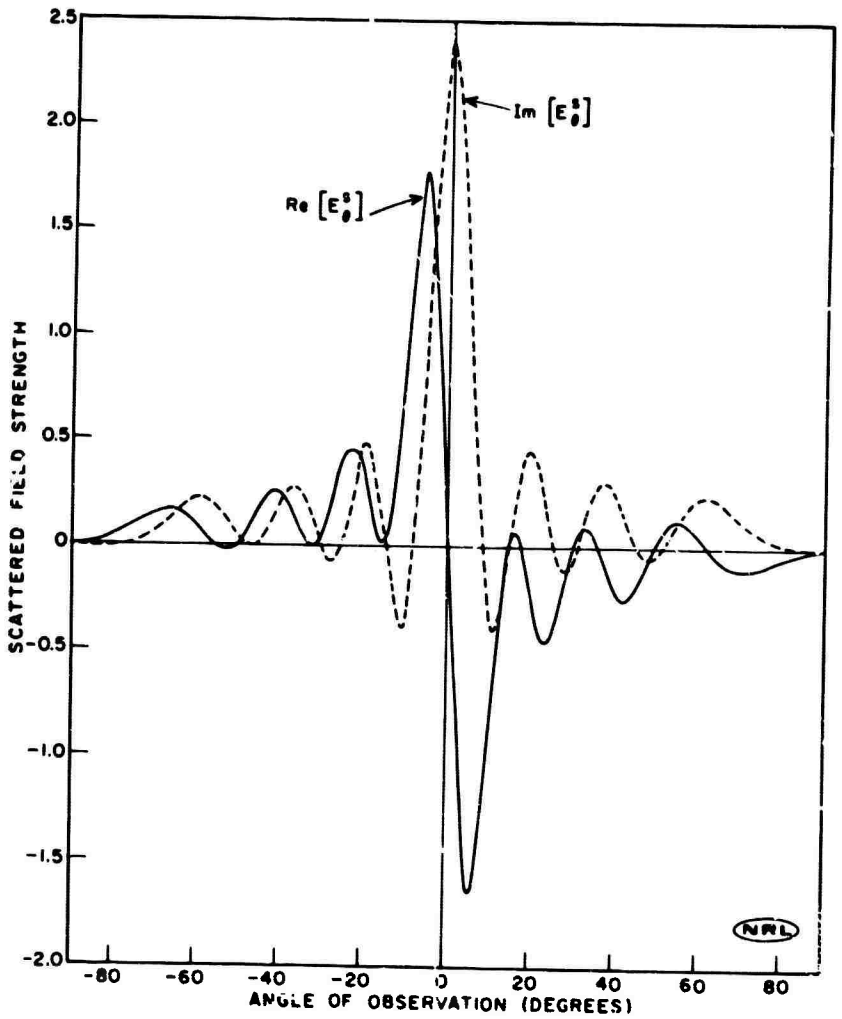

(a) Normal incidence; load impedance = 72 + j0 ohms; $\beta h = \pi/2$

Fig. 6 - The angular distribution of the in-phase and the phase-quadrature components of the *H*-plane scattered electric field (Continued)

$Re\left[E^s_\theta\right]$ = in-phase component of E^s_θ

$Im\left[E^s_\theta\right]$ = quadrature component of E^s_θ

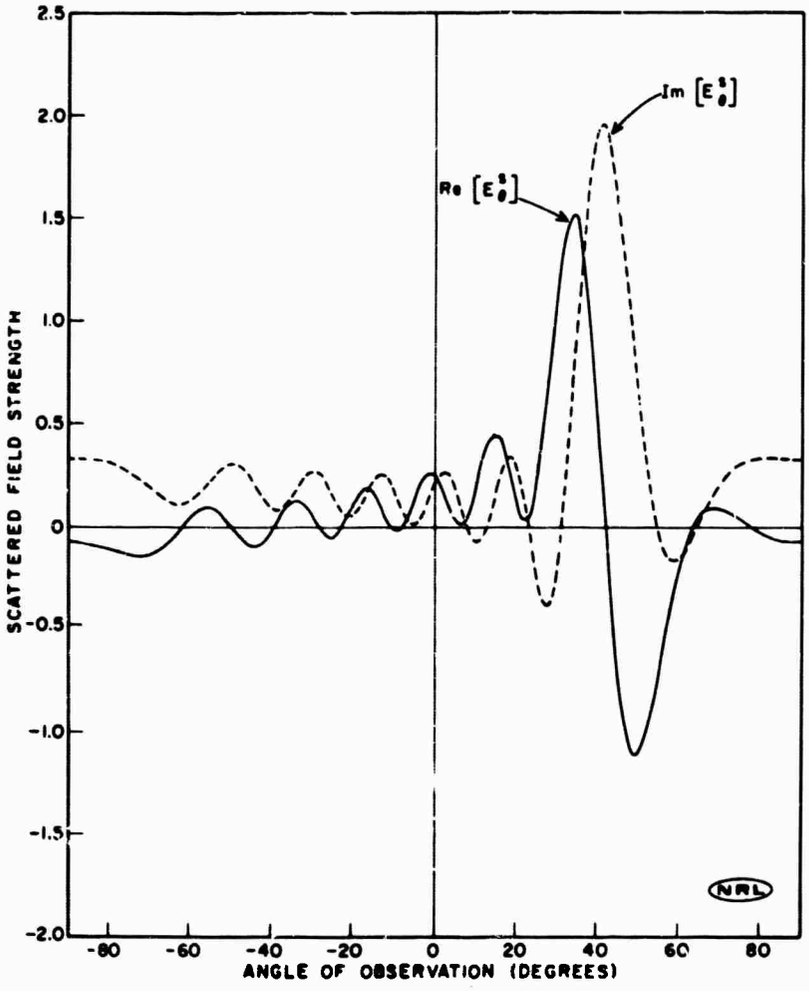

(b) Angle of incidence = -40 degrees; load impedance = 72 + j0 ohms; $\beta h = \pi/2$

Fig. 6 - The angular distribution of the in-phase and the phase-quadrature components of the *H*-plane scattered electric field (Continued)

$Re\left[E^s_\theta\right]$ = in-phase component of E^s_θ

$Im\left[E^s_\theta\right]$ = quadrature component of E^s_θ

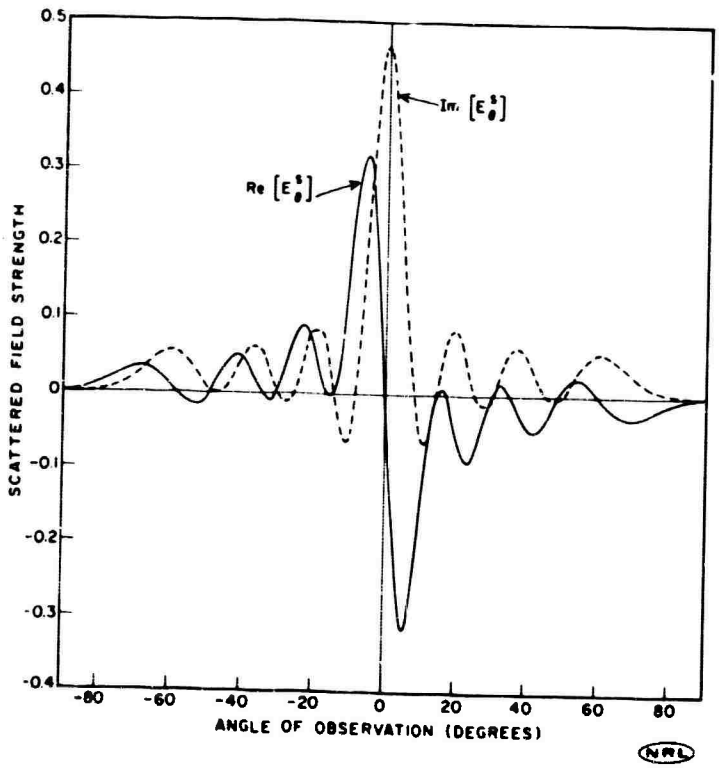

(c) Normal incidence; load impedance = 600 + j0 ohms; $\beta h = \pi/2$

Fig. 6 - The angular distribution of the in-phase and the phase-quadrature components of the *H*-plane scattered electric field

$Re\left[E_\theta^s\right]$ = in-phase component of E_θ^s

$Im\left[E_\theta^s\right]$ = quadrature component of E_θ^s

The Scattered Field Distribution in βh — In this section we present graphs which show how the amplitude and phase of the H-plane scattered electric field of the model array vary with the frequency of the illumination or the electrical half-length of the elements of the array. The direction of observation of the far-zone scattered field is chosen as either the reflected direction or the back-scattered direction. All the results presented in this section are calculated from Eq. (30).

In Fig. 7a we show the characteristics of the steady-state scattered field observed in the reflected direction for normal incidence and a nonreactive load impedance of 72 ohms. Note the element resonance at $\beta h = 1.58$ manifested by the maximum of the scattered-field strength. In Fig. 7b we present the βh characteristics of the reflected field for normal incidence and a certain type of reactive load impedance. Again we obtain a maximum of scattered field at $\beta h = 1.57$, where the elements resonate. In addition, a large resonance peak occurs at $\beta h = 3.64$, where evidently the reactance of the load resonates or tunes out the reactance of the impedance of the elements.

In Figs. 7a and 7b and in the figures to follow we find that the scattered field becomes quite weak for βh smaller than 0.40.

In Figs. 7c through 7f we show the field scattered in the reflected direction by the model array plotted versus the electrical half-length of the elements of the array. In Fig. 7c the central load impedance of the elements is a pure resistance of 600 ohms, and the illumination is incident normal to the plane of the array. The large load resistance appears to have obliterated the element resonance peak, leaving a slowly increasing amplitude of the scattered field with βh, except for a small dip at $\beta h = 3.2$. Figure 7e is similar to Fig. 7c, as might be expected, since only the angle of incidence of the illumination differs in the two figures. In Fig. 7d we present the field scattered by the model array of eight elements with nonreactive load impedances of 72 ohms when the illumination is incident at -40 degrees. The scattering characteristics exhibited resemble those for the same loading but with normal incidence, as shown in Fig. 7a. The element resonance appearing at $\beta h = 1.57$ is the salient feature of Fig. 7d.

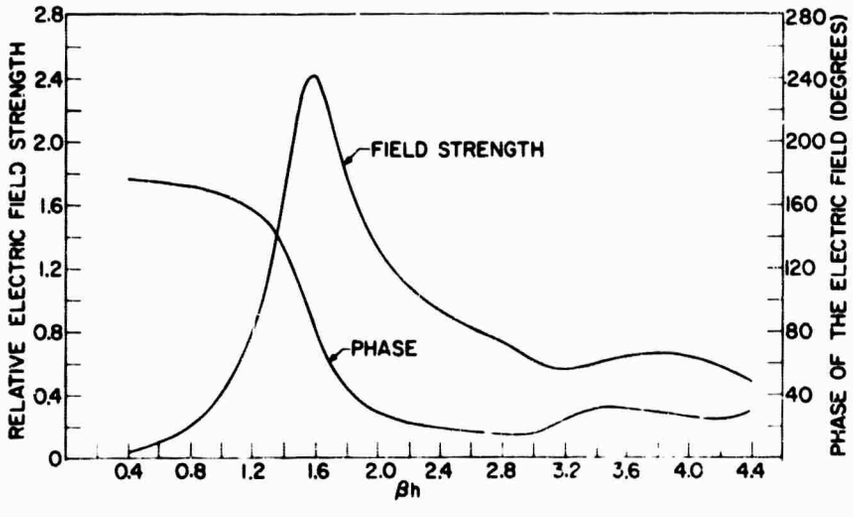

(a) Normal incidence; load impedance = 72 + j0 ohms

Fig. 7 - The H-plane scattered electric field observed in the reflected direction as a function of the electrical half-length of the elements of the array (Continued)

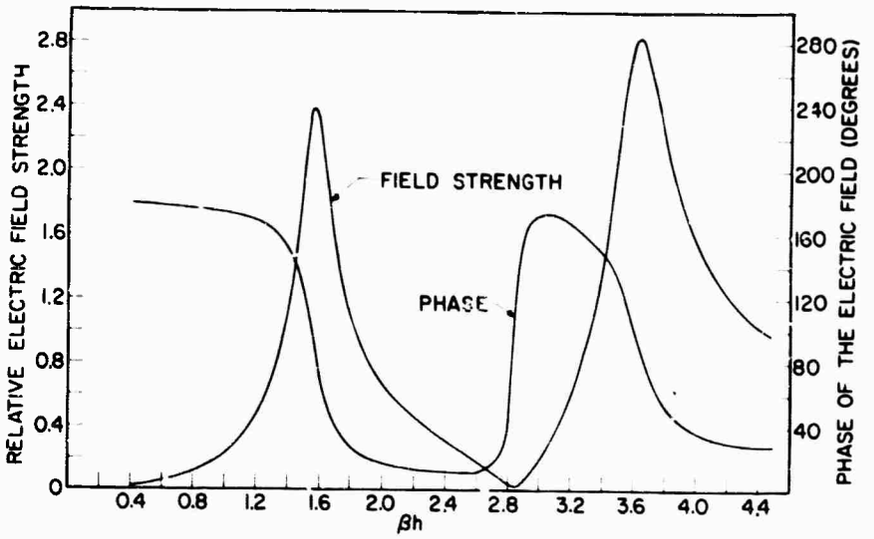

(b) Normal incidence; load impedance = 72 + j(300βh - 740/βh) ohms

(c) Normal incidence; load impedance = 600 + j0 ohms

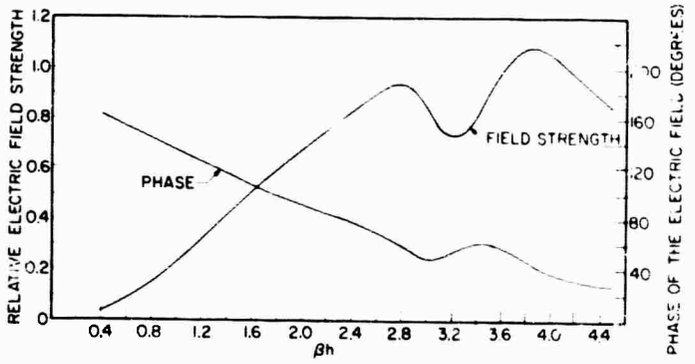

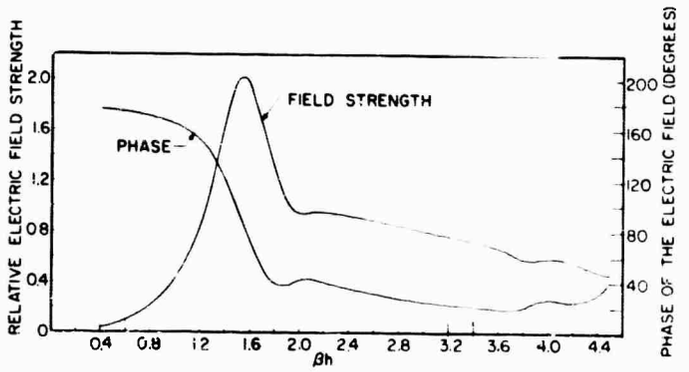

(d) Angle of incidence = -40 degrees; load impedance = 72 + j0 ohms

Fig. 7 - The *H*-plane scattered electric field observed in the reflected direction as a function of the electrical half-length of the elements of the array (Continued)

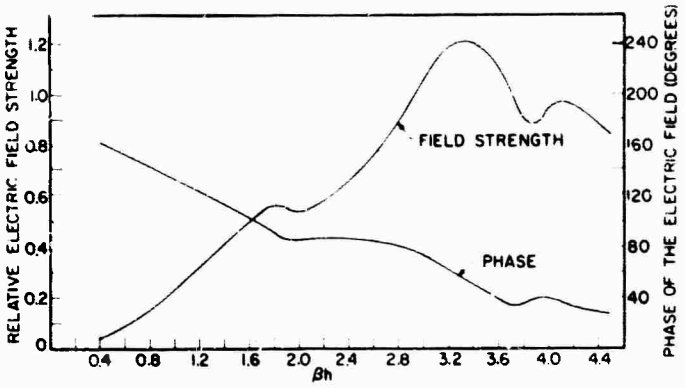

(e) Angle of incidence = -40 degrees; load impedance = 600 + j0 ohms

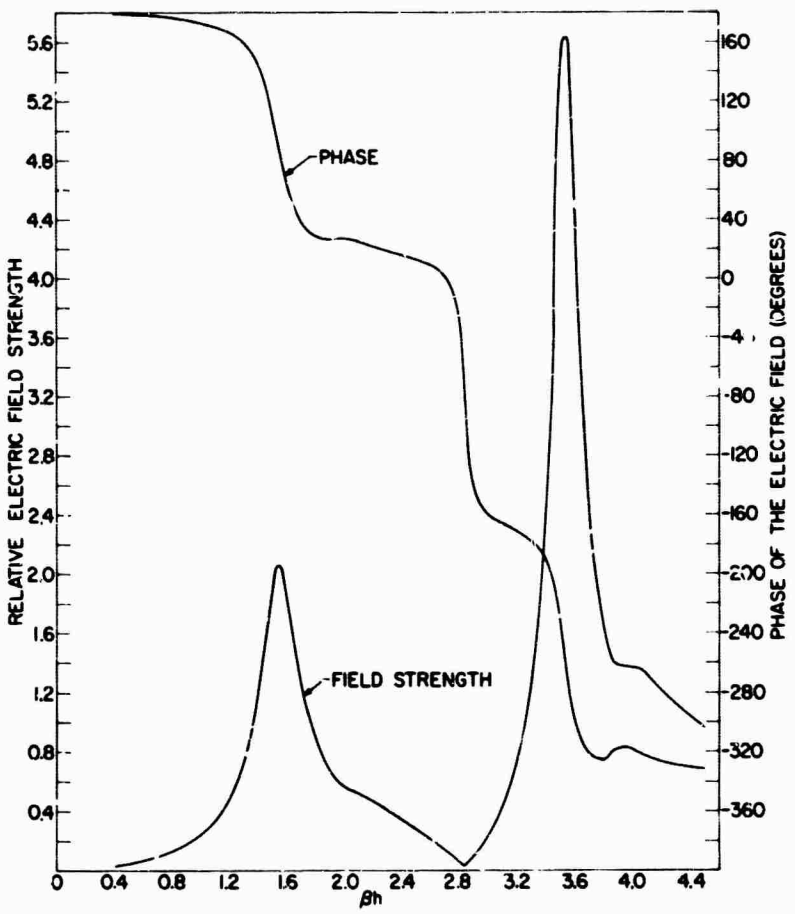

(f) Angle of incidence = -40 degrees; load impedance = 72 + j (30βh - 740/βh) ohms

Fi 7 - The *H*-plane scattered electric field observed in the reflected direction as a function of the electrical half-length of the elements of the array

Figure 7f shows the amplitude and phase of the field scattered in the reflected direction by the model array loaded with the indicated reactive impedances when the illuminating plane wave is incident on the array at -40 degrees. These characteristics closely resemble those shown in Fig. 7b over the interval 0.4 to 2.5 in βh. Intuitively, the similarity seems reasonable, because the two sets of curves give the scattering properties of the same array but at different angles of incidence of the illumination. However, in the range extending from 2.5 to 4.4 neither the amplitude nor the phase characteristic of Fig. 7f resembles closely the corresponding curve in Fig. 7b. An explanation of this divergence is unavailable. The fairly sharp peak at $\beta h = 1.57$ is, as usual, associated with the fundamental resonance of the elements of the array. The very high and narrow peak at $\beta h = 3.54$ comes about by virtue of the reactance of the load tuning out the reactance of the impedance of the elements of the array at the frequency corresponding to this value of βh.

We present in Fig. 8 the amplitude and phase of the electric field back-scattered by the model array with various load impedances at the element centers when illuminated by a plane electromagnetic wave incident at -40 degrees. In all three sets of back-scattering characteristics we have a large peak in the vicinity of $\beta h = 2.44$, where a first-order grating lobe occurs according to Eq. (33b). The results shown in the figure exhibit interference between the scattered-field components radiated by the individual elements of the array. The interference manifests itself by the appearance of the periodic minima in the amplitude of the field and the concurrent rather rapid advances in the phase of the scattered field. The interference effects naturally are absent in Fig. 7 because in the reflected direction the component scattered fields of the elements of the array are nearly in time phase with each other. In fact, the general nature of the βh characteristics of the H-plane scattered field observed in any direction can be explained best with the aid of Eq. (32). From Eq. (32) it is seen that the scattered field for a given load impedance and angle of incidence consists of two factors: the reflection factor $NG_{av} \exp[j(\gamma_1 + \pi/2)]$ and the interference factor $[\sin(N\psi/2)/N \sin(\psi/2)] \exp[j(N-1)\psi/2]$, where $\psi = \beta d(\sin\phi + \sin\phi_{inc})$. In the reflected direction, the scattered field becomes the reflection factor only, since in this direction the interference factor becomes unity. In directions other than the reflected direction, the effect of the interference factor appears along with the effect of the reflection factor. The magnitude of the interference factor is shown in Fig. 4 as the solid curve plotted versus $\psi/2$. As stated earlier, Eq. (32) does not give accurate results near the nulls of the interference factor, as indicated by the presence of minima instead of nulls in Fig. 8. However, the positions of the minima and of the grating lobes in Fig. 8 almost coincide with the locations of the nulls and grating lobes, respectively, of the interference factor. The amplitude curves of Figs. 8a and 8b resemble the general shape of the magnitude of the interference factor (see Fig. 4), except for some asymmetry introduced by the appropriate reflection factors shown in Figs. 7d and 7e. In Fig. 8c the element load impedances are reactive, and the amplitude characteristic does not resemble the magnitude of the interference factor. Figure 7f, portraying the corresponding reflection factor, accounts for the distortion. The high narrow peak at $\beta h = 3.55$ in Fig. 8c corresponds to a similar peak in Fig. 7f, where the reactance of the load tunes out the reactance of the element of the array.

SOME PARAMETERS OF A PLANE-POLARIZED LINEAR ARRAY OF CYLINDRICAL ELEMENTS DEDUCED FROM ITS SCATTERING PROPERTIES

Up to this point we have made a study of the H-plane scattered field of a linear array of cylindrical elements illuminated by a plane wave incident in the H plane of the array. In other words, we have been concerned with the problem of determining the scattered field given the character of the array and its illumination. Now, let us consider the inverse problem of the determination of some of the parameters of an unknown plane-polarized linear array of cylindrical elements from the character of its H plane scattered field and the known character of its incident illumination.

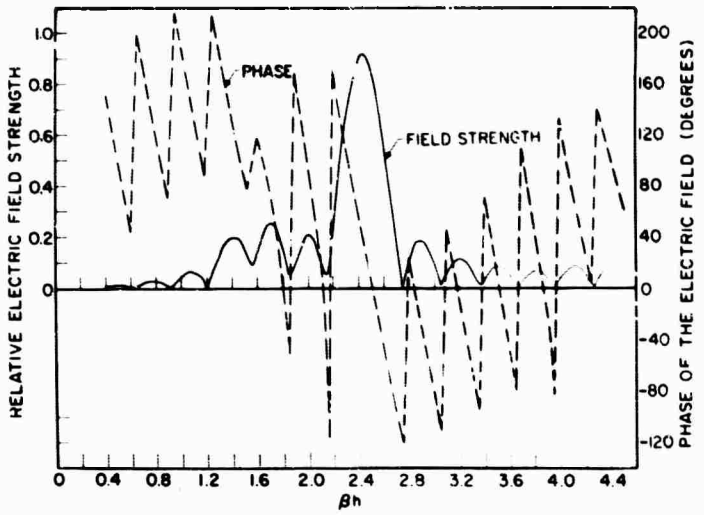

(a) Angle of incidence = -40 degrees;
load impedance = 72 + j0 ohms

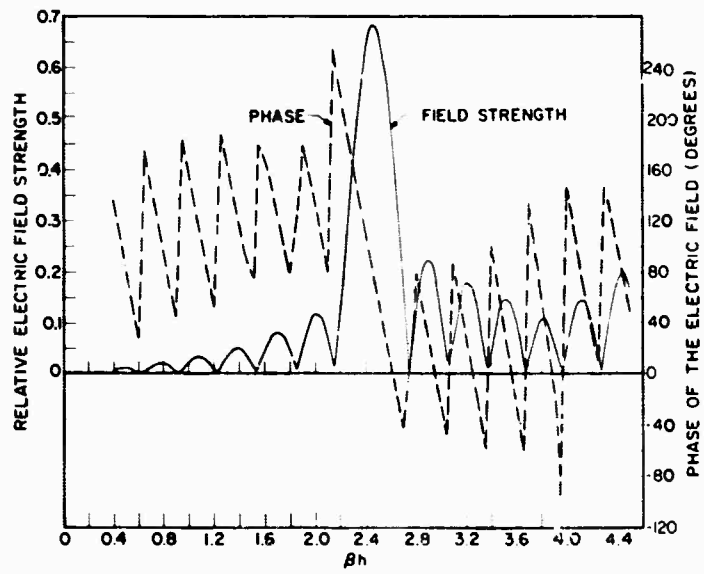

(b) Angle of incidence = -40 degrees;
load impedance = 600 + j0 ohms

Fig. 8 - The *H*-plane back-scattered electric field as a function of the electrical half-length of the elements of the array (Continued)

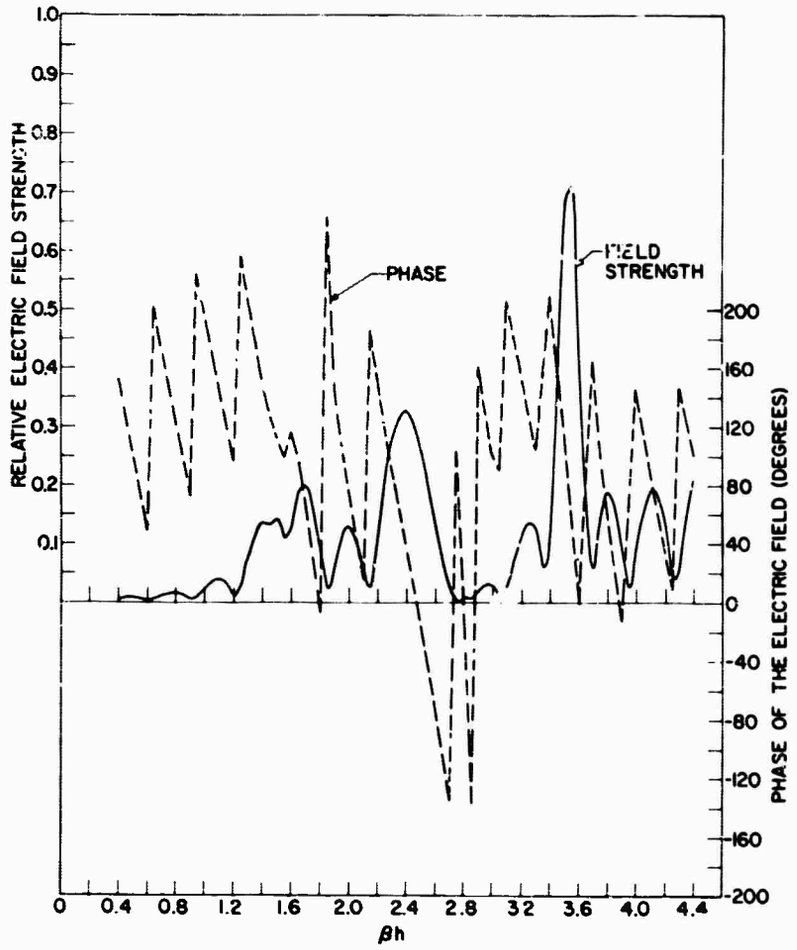

(c) Angle of incidence = -40 degrees; load impedance = 72 + j (300βh - 740/βh) ohms

Fig. 8 - The *H*-plane back-scattered electric field as a function of the electrical half-length of the elements of the array

Let us assume that the plane of the array is known; then one can determine the plane of polarization and, hence, the *H* plane of the array by the following well-known method. Illuminate the array with a linearly polarized plane wave, incident on the array at some convenient fixed angle of about 60 degrees or more. Rotate the plane of polarization of the incident wave and vary the frequency of the illumination until a sizable back-scattered field of the same polarization as the incident field is obtained. Now, with the frequency fixed, maximize the amplitude of the back-scattered field by further rotation-tuning of the plane of polarization of the incident wave. At this point, the plane of polarization of the array is approximately the same as that of the illumination.

Now that the *H* plane of the array, a plane orthogonal to the plane of polarization of the array, is determined, it is possible to deduce further information about the nature of the scattering array from the knowledge and information obtained from the study of the scattering properties of a linear array presented in the preceding sections of this report.

The further information about the array deducible from its scattering properties consists of the number of elements in the array, the interelement spacing, the H-plane radiation pattern, when used as a uniformly excited transmitting array, and, possibly, the fundamental resonant frequency of the elements of the array.

In the following determinations we assume an illumination-array setup like that shown in Fig. 1. The scattered field is examined only in the H plane of the array

As one continuously increases the frequency of the illumination of the array with a fixed angle of incidence of -40 degrees and $Z(\omega)$ for the load impedance of each element, the amplitude of the back-scattered field resembles that of Fig. 8a. It follows simply from Eqs. (33a) and (34) that the number of elements in the array is one plus the number of minima lying between successive grating lobes in the back-scattered field. From Figs. 8a and 8b, one observes that the scattering array has eight elements.

To determine the interelement spacing d, we make observations on the amplitude of the back-scattered field at the far-zone observation points P_1 and P_2 of Fig. 9. From point P_1 we illuminate the array from a direction ϕ_1 degrees from a reference direction with a plane electromagnetic wave and observe the amplitude of the back-scattered field at P_1 as the frequency of the illumination is scanned through several grating lobes spaced uniformly in frequency by an amount Δf_1. At point P_2 we repeat the experiment with ϕ_2 equal to ϕ_1 plus 90 degrees and find the grating lobes separated by a frequency increment Δf_2. It is easy to show from Eq. (33b) in conjunction with Fig. 9 that the element spacing d must satisfy the following transcendental relation:

$$\sin^{-1}[c/2\Delta f_1 d] + \sin^{-1}[c/2\Delta f_2 d] = \pi/2 . \tag{36}$$

For good accuracy the positions of the observation points P_1 and P_2 are chosen so that Δf_1 and Δf_2 do not differ by more than 50% of the smaller of the two frequency increments. The element spacing can be found from Eq. (36) by a well-known graphical technique.

With the number of elements and their spacing determined, it is a simple matter, from the theory of arrays, to find the H-plane radiation pattern of the linear array when used as a uniformly excited transmitting array at a given frequency.

When one measures the amplitude of the field scattered by the array in the reflected direction as a function of the frequency of the illumination, more than one resonance

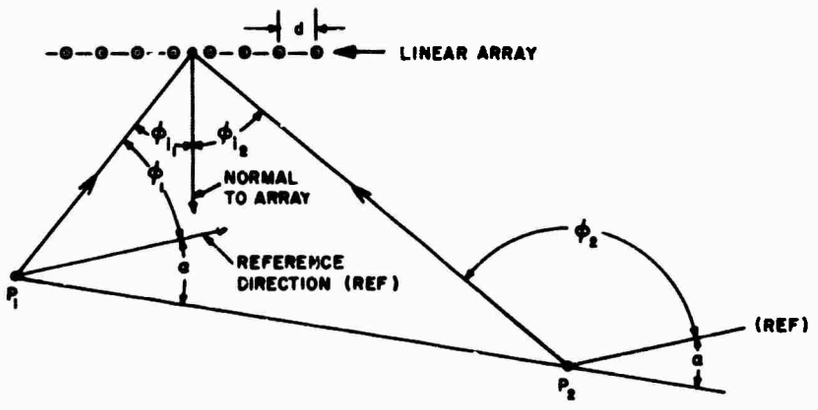

Fig. 9 - Arrangement for the determination of the element spacing of the array

makes an appearance, because the load impedance of the elements usually exhibits some reactance. Figures 7b and 7f show examples of this situation. To determine the resonant frequency of the elements from these reflection ω characteristics it becomes necessary to identify the element-resonance peak. Apparently from the figures cited above, the size of the element-resonance peak (at $\beta h = \pi/2$) changes, much less percentagewise than the other resonant peaks, associated with the reactance of the load, as the angle of incidence of the illumination undergoes a change from 0 to -40 degrees. With this criterion, we may determine the resonant frequency of the elements of the array, which is also the design frequency of the array. Whether this criterion for the selection of the element-resonance peak is reliable for various kinds of reactive loads can only be answered by further investigation.

CONCLUSIONS

A significant result of this investigation is the discovery that the H-plane scattered field of a linear array of cylindrical elements illuminated by a plane electromagnetic wave consists, to the first approximation, of two factors: a reflection factor and an interference factor. The interference factor, defined as

$$\frac{\sin (N\psi/2)}{\sin (\psi/2)} \exp[j(N-1)\psi/2] ,$$

where $\psi = \beta d(\sin\phi + \sin\phi_{inc})$, is of the same form as the array factor of a uniform linear array of N elements excited with uniform amplitude and element-to-element phase progression. In the reflected direction, where $\phi = -\phi_{inc}$ and ψ vanishes, the scattered field becomes equal to the reflection factor, since the interference factor becomes unity. More physically speaking, the components of the scattered field contributed by the individual elements of the array are in time phase in the reflected direction. The reflection factor is calculated from an approximation technique incorporating the set of integral equations characterizing the array and the incident illumination. It follows that the reflection factor is a function of the electrical half-length of the elements, the electrical spacing of the elements, the load impedance, and the angle of incidence of the illumination. With the aid of the interference factor of the approximate formula for the scattered field, it is possible to discern much about the nature of the H-plane scattered field, for example, the positions of the grating lobes and the minima of the scattering pattern for various plane-wave illuminations.

From the scattering characteristics of a passive linear array of cylindrical elements, one can deduce its plane of polarization, the number of elements in the array, the interelement spacing of the array, the H-plane radiation pattern of the array, when used as a uniformly excited transmitting array, and, possibly, the resonant frequency of the elements of the array.

No doubt the technique described in this report for the calculation of the scattered field of a linear array can be extended to the study of the scattering properties of planar arrays of cylindrical elements.

ACKNOWLEDGMENTS

The author is indebted to John P. Barry for helpful discussions in connection with this study and for his aid in setting up the initial numerical calculations. The effort of Jon D. Wilson in developing all the computer programs used in this investigation is especially appreciated by the author.

REFERENCES

1. King, R.W.P., and Wu, T.T., "The Scattering and Diffraction of Waves," Cambridge: Harvard University Press, 1959

2. Chen, K.M., and Liepa, V., "The Minimization of the Back Scattering of a Cylinder by Central Loading," IEEE Trans. Antennas and Propagation AP-12 (No. 5):576-582 (1964)

3. Garbacz, R.J., "Determination of Antenna Parameters by Scattering Cross-Section Measurements," Proc. IEE 111(No. 10):1679-1686 (1964)

4. Ramo, S., Whinnery, J.R., and Van Duzer, T., "Fields and Waves in Communication Electronics," New York:Wiley, pp. 259-266, 1965

5. King, R.W.P., "The Linear Antenna - Eighty Years of Progress," Proc. IEEE 55(No. 1):2-16 (1967)

Appendix A

THE EVALUATION OF THE APPROXIMATION TECHNIQUE OF CALCULATING THE CURRENTS INDUCED IN AN ARRAY BY AN INCIDENT PLANE WAVE

To test the induced currents calculated using Eqs. (20) and (21) for a given angle of incidence, array loading, and value of βh, we substitute the current coefficients $\mathfrak{A}_i$ and $\mathfrak{B}_i$ into the set of integral equations of the array, Eq. (19), and compare the complex values of the right and left members of each equation of the set for various values of βz. In Table A1, we present some examples of the comparison of the right and left members of the set of equations (19). The percentage magnitude difference is defined as 100 times the ratio of the absolute value of the difference between the magnitudes of the right and left members to the average of the two magnitudes. The symbol m designates the equation associated with the m-th element of the array.

Graphs of the percentage magnitude difference and the absolute value of the angle difference, both averaged over the array, as well as the normalized current amplitude of the fourth element are shown in Fig. A1 plotted versus the position along the array elements. It is assumed for this discussion that the normalized-current amplitude distributions do not change appreciably from element to element in the array or with the angle of incidence. For a given value of βh, it is observed from both the table and the graphs that the margin by which the calculated currents fail to satisfy Eq. (19) is in general, greatest for the larger load impedances and angles of incidence. The graphs also show in general that the margin of failure to satisfy Eq. (19) becomes large in the regions where the normalized current amplitude is small. An exception occurs in the case of $\beta h = 3.0$, where the margin of failure to satisfy becomes fairly large in the vicinity of $\beta z = 0$ for the larger load impedances, although the current is large in this region. Since the amplitude of the electromagnetic field radiated by a given differential length within a cylindrical element varies linearly with the amplitude of the current in the elementary length, it follows that one should obtain a more realistic error criterion, as far as the scattered field is concerned, if both the percentage magnitude difference and the angle difference are multiplied at each point in βz by the normalized current amplitude as a weighting factor. Because of this weighting factor, the large margins of failure to satisfy Eq. (19), which occur in low-current regions of βz, do not introduce large errors when one calculates the scattered field of an array with the numerical approximation technique described in this report.

Needless to say, this method of evaluation of our approximation leaves much to be desired. A much more worthwhile evaluation can be made by comparing the calculated results with either the experimental or theoretical results of other research workers. Unfortunately, such results are not available at present in the antenna literature as far as the author has been able to determine from a limited amount of literature search.

Table A1

The Degree to Which the Calculated Array Currents Fail to Satisfy the Set of Integral Equations of the Model Array at Various Points along the Length of the Elements

n	Magnitude Difference (%)	Angle Difference (degrees)
$\beta A = 1.5$; $\beta s = 1.2$; $Z = 72 + j0$ ohms; $\phi_{inc} = -40$ degrees		
1	1.4	5.1
2	1.1	2.5
3	2.2	2.5
4	3.2	2.7
5	3.2	3.3
6	2.2	3.5
7	1.4	3.0
8	2.0	2.0
$\beta A = 1.5$; $\beta s = 1.2$; $\phi_{inc} = 0$ degrees; $Z = 72 + j0$ ohms		
1	3.7	3.0
2	6.0	2.4
3	5.2	2.7
4	5.5	2.6
---------- line of symmetry ----------		
$\beta A = 1.5$; $\beta s = 1.2$; $\phi_{inc} = 0$ degrees; $Z = 600 + j0$ ohms		
1	12.2	2.4
2	14.3	1.8
3	14.0	3.0
4	13.8	2.0
---------- line of symmetry ----------		
$\beta A = 1.5$; $\beta s = 1.2$; $\phi_{inc} = -40$ degrees; $Z = 600 + j0$ ohms		
1	14.4	9.4
2	8.0	5.9
3	7.7	3.9
4	9.5	3.2
5	12.0	3.1
6	13.5	5.2
7	8.6	5.7
8	7.7	4.4
$\beta A = 1.5$; $\beta s = 1.2$; $\phi_{inc} = 0$ degrees; $Z = 72 - j(43.5)$ ohms		
1	3.7	3.5
2	6.6	2.8
3	5.2	3.1
4	5.8	3.0
---------- line of symmetry ----------		
$\beta A = 3.0$; $\beta s = 2.5$; $\phi_{inc} = 0$ degrees; $Z = 72 + j0$ ohms		
1	1.8	10.3
2	2.9	7.9
3	2.8	6.6
4	2.8	6.2
---------- line of symmetry ----------		
$\beta A = 3.0$; $\beta s = 2.5$; $\phi_{inc} = -40$ degrees; $Z = 72 + j0$ ohms		
1	9.8	16
2	10.6	20.9
3	13.6	22.0
4	15.5	19.2
5	12.5	20.0
6	11.8	20.1
7	15.3	20.4
8	5.8	20.0

n	Magnitude Difference (%)	Angle Difference (degrees)
$\beta A = 3.0$; $\beta s = 2.5$; $\phi_{inc} = 0$ degrees; $Z = 600 + j0$ ohms		
1	12.8	2.3
2	9.6	2.2
3	8.3	1.5
4	7.6	1.2
---------- line of symmetry ----------		
$\beta A = 3.0$; $\beta s = 2.5$; $\phi_{inc} = -40$ degrees; $Z = 800 + j0$ ohms		
1	14.0	1.4
2	16.3	2.0
3	16.0	2.1
4	18.0	2.1
5	18.0	2.1
6	16.1	2.1
7	15.9	2.2
8	16.6	1.0
$\beta A = 3.0$; $\beta s = 0$; $\phi_{inc} = -40$ degrees; $Z = 800 + j0$ ohms		
1	11.8	5.9
2	13.2	7.1
3	13.9	6.8
4	13.5	8.7
5	13.7	6.8
6	13.5	8.9
7	13.1	8.7
8	13.2	7.5
$\beta A = 3.0$; $\beta s = 0$; $\phi_{inc} = 0$ degrees; $Z = 72 + j(653)$ ohms		
1	14.7	8.3
2	16.7	6.9
3	18.7	6.6
4	18.7	6.6
---------- line of symmetry ----------		
$\beta A = 3.0$; $\beta s = 0$; $\phi_{inc} = -40$ degrees; $Z = 72 + j(653)$ ohms		
1	12.4	10.4
2	13.2	13.1
3	13.0	14.0
4	13.0	13.0
5	13.0	13.3
6	13.7	13.1
7	13.1	13.2
8	14.5	12.5

(a) βh = 1.5; Z = 72 + j0 ohms

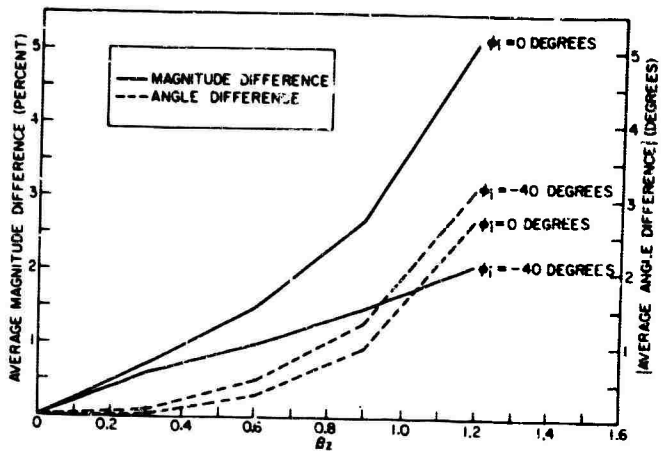

(b) βh = 1.5; Z = 72 - j43.5 ohms

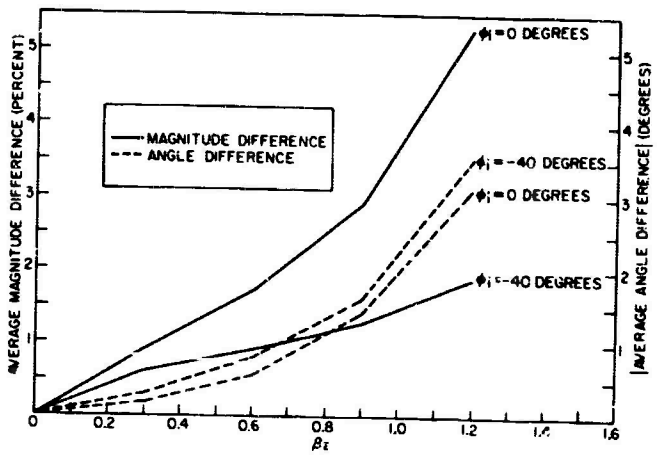

(c) βh = 1.5; Z = 600 + j0 ohms;
ϕ_{inc} = 0 degree

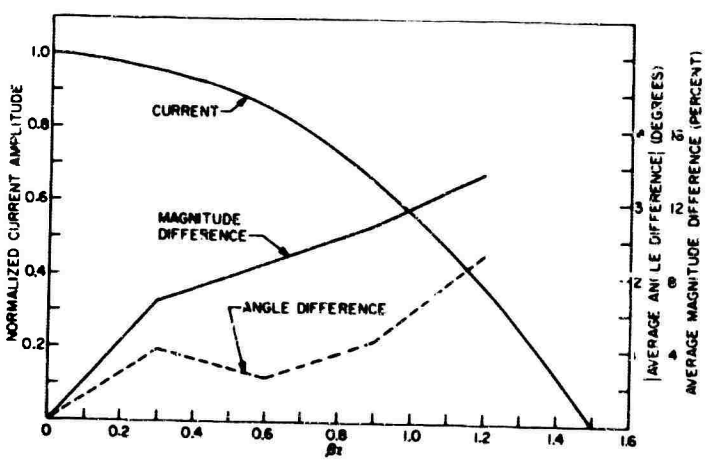

Fig. A1 - The magnitude difference and the absolute value of the angle difference, both averaged over the array, shown as functions of position along the length of the elements of the model array (Continued)

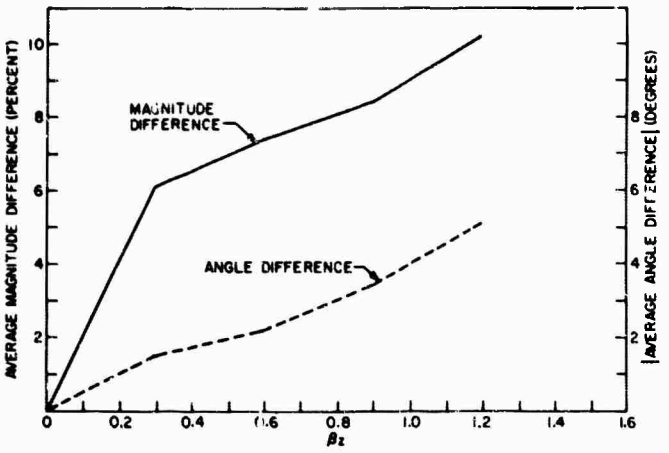

(d) $\beta\lambda$ = 1.5; Z = 600 + j0 ohms; ϕ_{inc} = -40 degrees

(e) $\beta\lambda$ = 3.0; Z = 72 + j0 ohms

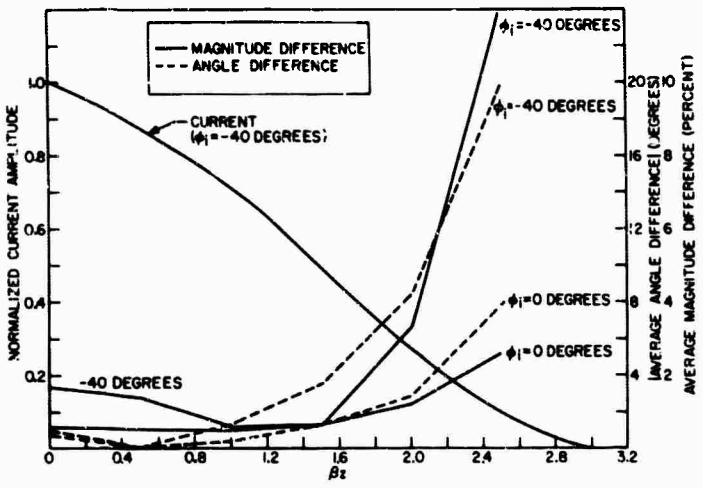

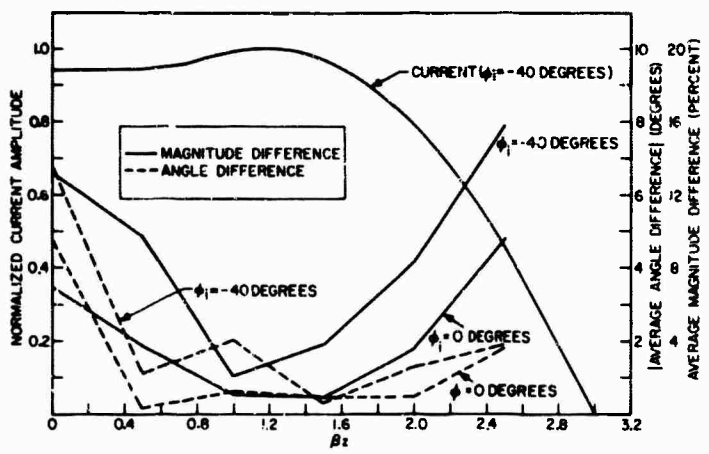

(f) $\beta\lambda$ = 3.0; Z = 600 + j0 ohms

Fig. A1 - The magnitude difference and the absolute value of the angle difference, both averaged over the array, shown as functions of position along the length of the elements of the model array (Continued)

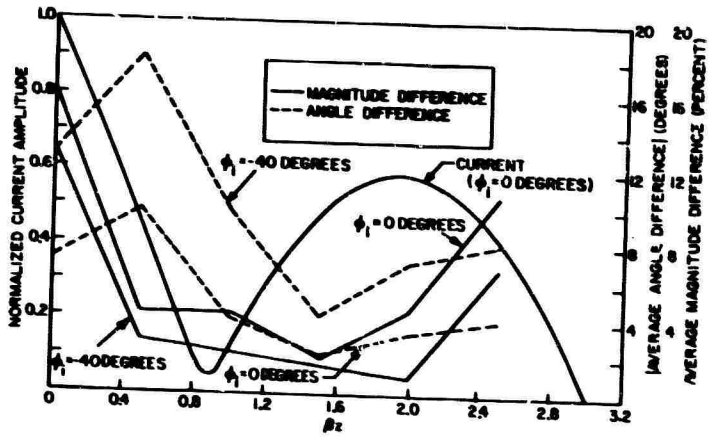

(g) $\beta\lambda$ = 3.0; Z = 72 + j653 ohms

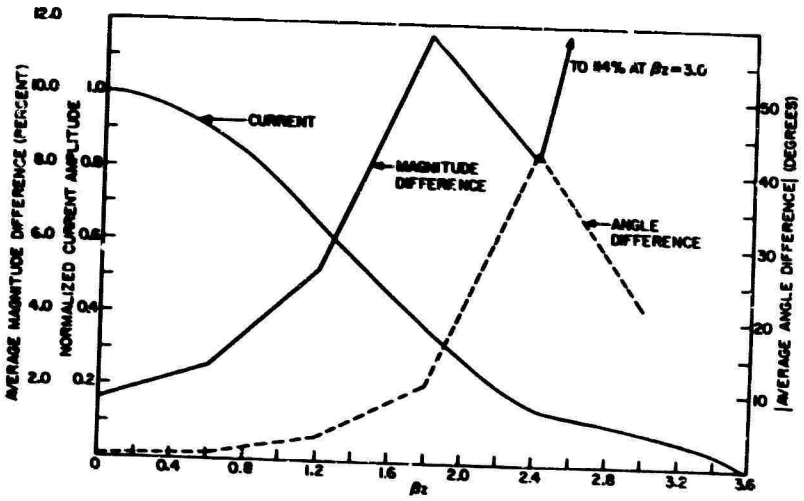

(h) $\beta\lambda$ = 3.6; Z = 7 j0 ohms; ϕ_{inc} = 0 degree

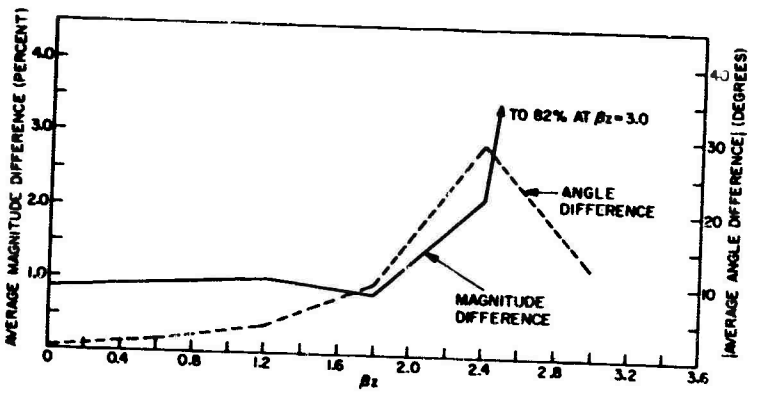

(i) $\beta\lambda$ = 3.6; Z = 72 + j0 ohms; ϕ_{inc} = -40 degrees

Fig. A1 - The magnitude difference and the absolute value of the angle difference, both averaged over the array, shown as functions of position along the length of the elements of the model array (Continued)

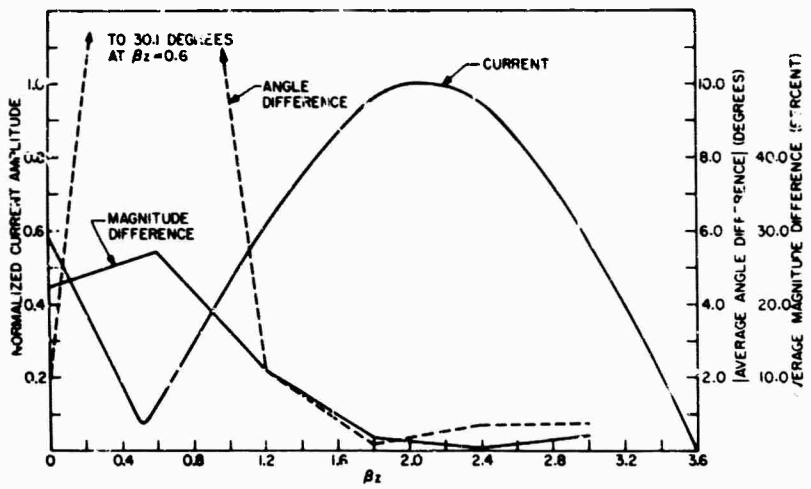

(j) βh = 3.6; Z = 72 + j874 ohms; ϕ_{inc} = -40 degrees

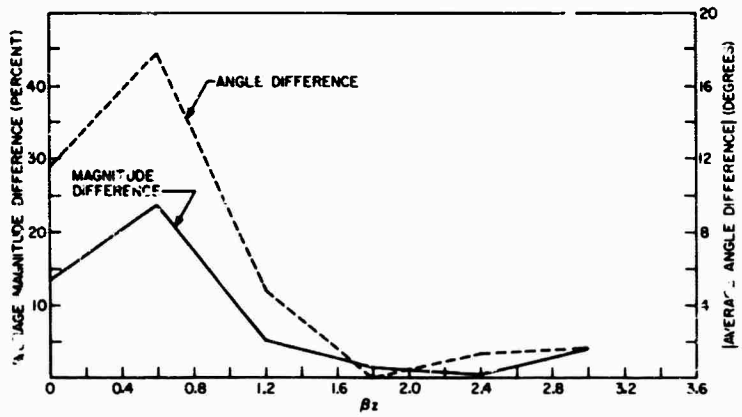

(k) βh = 3.6; Z = 72 + j874 ohms; ϕ_{in} = 0 degree

Fig. A1 - The magnitude difference and the absolute value of the angle difference, both averaged over the array, shown as functions of position along the length of the elements of the model array (Continued)

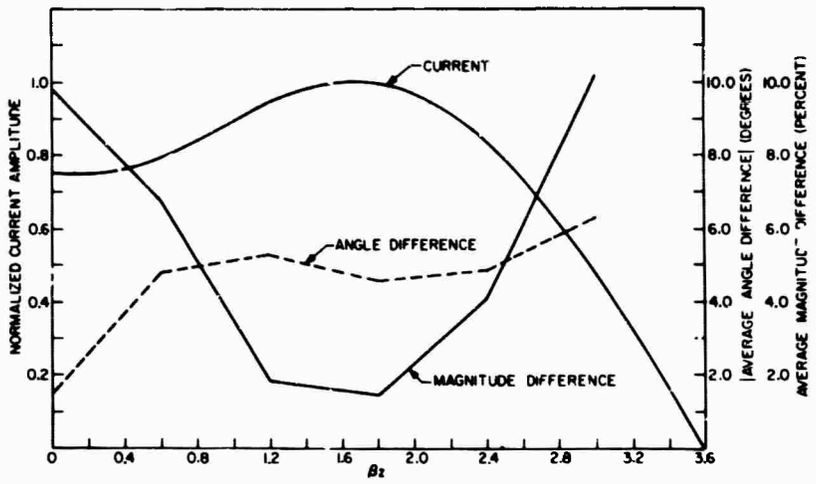

(l) $\beta\lambda$ = 3.6; Z = 600 + j0 ohms; ϕ_{inc} = 0 degree

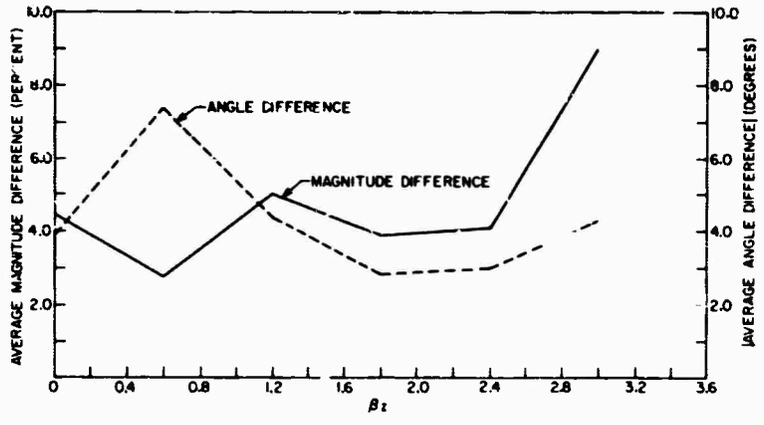

(m) $\beta\lambda$ = 3.6; Z = 600 + j0 ohms; ϕ_{inc} = -40 degrees

Fig. A1 - The magnitude difference and the absolute value of the angle difference, both averaged over the array, shown as functions of position along the length of the elements of the model array

Appendix B

THE AMPLITUDE AND PHASE OF THE EFFECTIVE SCATTERING COEFFICIENT OF THE ELEMENTS OF THE MODEL ARRAY

We list in Table B1 the amplitude G_i and the phase γ_i of the effective scattering coefficient of the i-th element of the model array, where i runs from one to eight. In these tabulations DFA means the deviation from the average and DFδ means the deviation from δ, where $\delta = \beta d \sin \phi_{inc}$ (see Eq. (31) of the text). At the bottom of each table for normal incidence, we show the rms value of the percent DFA of the G_i and the rms value of the DFA of the γ_i both taken over the array. In the case of incidence at -40 degrees, the rms value of the DFδ of $\Delta\gamma_i$ is given.

The tables bear out the statement made in the text that the values of G_i remain approximately invariant over the array and the γ_i approximately linear along the array. Tables B1 (k), B1 (l), and B1 (n) exhibit the largest deviation from this condition because they involve the resonances at $\beta A = \pi/2$ and near $\beta A = 3.6$. Note that the element resonance has little effect when the load impedance is 600 ohms as in Tables B1 (q) and B1 (r).

Table B1
The Amplitude and Phase of the Effective Scattering Coefficient of the Elements of the Model Array

i	G_i	DFA of G_i (%)	γ_i (degrees)	DFA of γ_i (degrees)	$\Delta\gamma_i$ (degrees)	DFδ of $\Delta\gamma_i$ (degrees)
(a) $z = 72 + j0$ ohms; $\beta A = 1.0$; $\phi_{inc} = 0$ degree						
1	0.0522	3.0	77.0	-0.1	—	—
2	0.0503	-1.0	76.5	-0.6	—	—
3	0.0495	-3.0	78.0	0.9	—	—
4	0.0508	1.0	77.1	0.0	—	—
---------- line of symmetry ----------						
5	0.0508	1.0	77.1	0.0	—	--
6	0.0495	-3.0	78.0	0.9	—	—
7	0.0503	-1.0	76.5	-0.6	—	—
8	0.0522	3.0	77.0	-0.1	—	—
rms value	—	2.24	—	0.543	—	—

(Table B1 continues)

Table B1 (Continued)

i	G_i	DFA of G_i (%)	γ_i (degrees)	DFA of γ_i (degrees)	$\Delta\gamma_i$ (degrees)	DFδ of $\Delta\gamma_i$ (degrees)
(b) Z = 72 + j0 ohms; βh = 1.0; ϕ_{inc} = -40 degrees						
1	0.0532	2.1	78.6	—	-76.5	-2.8
2	0.0535	2.7	2.1	—	-74.5	-0.8
3	0.0529	1.5	-72.4	—	-74.9	-1.2
4	0.0523	0.4	-147.3	—	-72.9	0.8
5	0.0511	-1.9	-220.2	—	-74.0	-0.3
6	0.0512	-1.7	-294.2	—	-71.9	1.8
7	0.0503	-3.4	-366.1	—	-75.2	-1.5
8	0.0520	-0.2	-441.3	—	—	—
rms value	—	2.00	—	—	—	1.52
(c) Z = 300 + j0 ohms; βh = 1.0; ϕ_{inc} = 0 degree						
1	0.0417	2.2	56.6	-0.5	-	—
2	0.0404	-1.0	56.8	-0.3	—	—
3	0.0403	-1.2	58.1	1.0	—	—
4	0.0408	0.0	57.1	0.0	—	—
---------- line of symmetry ----------						
rms value	—	1.35	—	0.579	—	—
(d) Z = 300 + j0 ohms; βh = 1.0; ϕ_{inc} = -40 degrees						
1	0.0427	3.4	57.6	—	-76.0	-2.3
2	0.0422	2.2	-18.4	—	-74.1	-0.4
3	0.0417	1.5	-92.5	—	-74.4	-0.7
4	0.0411	0.0	-166.9	—	-72.7	1.0
5	0.0406	-1.2	-239.6	—	-73.9	-0.2
6	0.0406	-1.2	-313.5	—	-72.1	1.6
7	0.0404	-1.7	-385.6	—	75.5	-1.8
8	0.0411	0.0	-461.1	—	—	—
rms value	—	1.75	—	—	—	1.35

(Table B1 continues)

Table B1 (Continued)

i	G_i	DFA of G_i (%)	γ_i (degrees)	DFA of γ_i (degrees)	$\Delta\gamma_i$ (degrees)	DFδ of $\Delta\gamma_i$ (degrees)
(e) Z = 600 + j0 ohms; βh = 1.0; ϕ_{inc} = 0 degree						
1	0.0294	1.4	45.0	-0.6	—	—
2	0.0287	-1.0	45.4	-0.2	—	—
3	0.0288	-0.7	46.3	0.7	—	—
4	0.0290	0.0	45.0	0.0	—	—
---------- line of symmetry ----------						
rms value	—	0.929	—	0.472	—	—
(f) Z = 600 + j0 ohms; βh = 1.0; ϕ_{inc} = -40 degrees						
1	0.0299	2.8	45.6	—		
					-75.3	-1.6
2	0.0296	1.7	-29.7	—		
					-73.9	-0.2
3	0.0293	0.7	-103.6	—		
					-74.0	-0.3
4	0.0289	-0.7	-177.6	—		
					-72.9	0.8
5	0.0287	-1.4	-250.5	—		
					-73.9	-0.2
6	0.0287	-1.4	-324.4	—		
					-72.5	1.2
7	0.0287	-1.4	-396.9	—		
					-75.1	-1.4
8	0.0290	-0.3	-472.0	—	—	—
rms value	—	1.49	—	—	—	0.845
(g) Z = 72 + j0 ohms; βh = 3.6; ϕ_{inc} = 0 degree						
1	0.0823	1.4	-63.1	-4.4	—	—
2	0.0798	-1.7	-59.5	-0.8	—	—
3	0.0807	-0.6	-56.8	1.9	—	—
4	0.0820	1.0	-55.5	3.2	—	—
---------- line of symmetry ----------						
rms value	—	1.25	—	2.91	—	—

(Table B1 continues)

Table B1 (Continued)

i	G_i	DFA of G_i (%)	γ_i (degrees)	DFA of γ_i (degrees)	$\Delta\gamma_i$ (degrees)	DFδ of $\Delta\gamma_i$ (degrees)
(h) Z = 72 + j0 ohms; βh = 3.6; ϕ_{inc} = -40 degrees						
1	0.0817	-3.7	-71.9	—		
					-263.6	-2.9
2	0.0873	3.0	-335.5	—		
					-267.6	3.7
3	0.0867	2.2	-603.1	—		
					-264.6	-0.4
4	0.0853	0.6	-867.7	—		
					-265.8	1.0
5	0.0851	0.4	-1133.5	—		
					-264.5	-0.2
6	0.0824	-2.8	-1398.0	—		
					-262.7	-3.8
7	0.0826	-2.6	-1660.7	—		
					-262.9	-4.0
8	0.0871	2.7	-1923.6	—	—	—
rms value	—	2.50	—	—	—	1.74
(i) Z = 600 + j0 ohms; βh = 3.6; ϕ_{inc} = 0 degree						
1	0.128	3.4	-38.1	-6.6	—	—
2	0.121	-2.3	-32.9	-1.4	—	—
3	0.122	-1.5	-28.7	2.8	—	—
4	0.124	0.2	-26.4	5.1	—	—
---------- line of symmetry ----------						
rms value	—	2.19	—	4.45	—	—
(j) Z = 600 + j0 ohms; βh = 3.6; ϕ_{inc} = -40 degrees						
1	0.132	-5.0	-51.5	—		
					-262.3	1.6
2	0.144	3.6	-313.8	—		
					-268.9	-2.4
3	0.145	4.3	-582.7	—		
					-264.8	0.6
4	0.141	1.4	-847.5	—		
					-266.2	-0.6
5	0.141	1.4	-1113.7	—		
					-265.0	0.7
6	0.135	-2.9	-1378.7	—		
					-261.4	2.5
7	0.132	-5.0	-1640.1	—		
					-261.2	2.3
8	0.142	2.2	-1901.3	—	—	—
rms value	—	3.51	—	—	—	2.77

(Table B1 continues)

Table B1 (Continued)

i	G_i	DFA of G_i (%)	γ_i (degrees)	DFA of γ_i (degrees)	$\Delta\gamma_i$ (degrees)	DFδ of $\Delta\gamma_i$ (degrees)
(k) $Z = 72 + j[300\beta h - (740/\beta h)]$ ohms; $\beta h = 3.6$; $\phi_{inc} = 0$ degree						
1	0.390	10.0	-2.9	-13.9	—	—
2	0.340	-4.1	6.5	-4.5	—	—
3	0.336	-5.2	17.4	6.4	—	—
4	0.352	-0.7	23.0	12.0	—	—
---------- line of symmetry ----------						
rms value	—	6.01	—	10.22	—	—
(l) $Z = 72 + j[300\beta h - (740/\beta h)]$ ohms; $\beta h = 3.6$; $\phi_{inc} = -40$ degrees						
1	0.480	-8.9	-33.5	—		
					-258.4	-6.8
2	0.567	7.6	-291.1	—		
					-273.2	8.0
3	0.587	11.4	-565.1	—		
					-264.9	-0.3
4	0.554	5.1	-830.0	—		
					-267.1	1.9
5	0.558	5.9	-1097.1	—		
					-266.4	1.2
6	0.505	-4.2	-1363.5	—		
					-258.4	-6.8
7	0.458	-13.1	-1621.9	—		
					-254.8	-10.4
8	0.508	-3.6	-1876.7	—	—	—
rms value	—	8.13	—	—	—	6.21
(m) $Z = 72 + j0$ ohms; $\beta h = \pi/2$; $\phi_{inc} = 0$ degree						
1	0.278	-7.0	-7.1	-4.3	—	—
2	0.313	4.7	-0.5	2.3	—	—
3	0.300	0.3	-2.2	0.6	—	—
4	0.305	2.0	-1.6	1.2	—	—
---------- line of symmetry ----------						
rms value	—	4.34	—	2.53	—	—

(Table B1 continues)

Table B1 (Continued)

i	G_i	DFA of G_i (%)	γ_i (degrees)	DFA of γ_i (degrees)	$\Delta\gamma_i$ (degrees)	DFδ of $\Delta\gamma_i$ (degrees)
(n) Z = 72 + j0 ohms; $\beta h = \pi/2$; ϕ_{inc} = -40 degrees						
1	0.289	16.5	-21.2	—	-110.7	5.0
2	0.233	-6.0	-131.9	—	-109.5	6.2
3	0.240	-3.2	-241.4	—	-115.5	0.2
4	0.258	4.0	-356.9	-	-118.8	-3.1
5	0.265	6.8	-475.7	—	-118.7	-3.0
6	0.255	2.8	-594.4	—	-115.3	0.4
7	0.233	-6.0	-709.7	—	-104.8	10.9
8	0.213	-14.1	-814.5	—	—	—
rms value	—	8.83	—	—	—	5.24
(o) Z = 300 + j0 ohms; $\beta h = \pi/2$; ϕ_{inc} = 0 degree						
1	0.105	-2.0	-3.0	-1.95	—	—
2	0.109	2.0	0.3	1.35	—	—
3	0.107	0.0	-1.0	0.05	—	—
4	0.108	1.0	-0.5	0.55	—	—
---------- line of symmetry ----------						
rms value	—	1.50	—	1.22		—
(p) Z = 300 + j0 ohms; $\beta h = \pi/2$; ϕ_{inc} = -40 degrees						
1	0.109	8.4	-8.6	—	-114.7	1.0
2	0.0986	-1.6	-123.3	—	-112.5	3.2
3	0.0974	-3.6	-235.8	—	-114.4	1.3
4	0.101	0.4	-350.2	—	-117.0	-1.3
5	0.104	3.4	-467.2	—	-118.0	-2.3
6	0.104	3.4	-585.2	—	-116.5	-0.8
7	0.0985	-2.6	-701.7	—	-111.4	4.3
8	0.0932	-7.6	-813.1	—	—	—
rms value	—	4.66	—	—	—	2.36

(Table B1 continues)

Table B1 (Continued)

i	G_i	DFA of G_i (%)	γ_i (degrees)	DFA of γ_i (degrees)	$\Delta\gamma_i$ (degrees)	DFδ of $\Delta\gamma_i$ (degrees)
(q) Z = 600 + j0 ohms; $\beta h = \pi/2$; ϕ_{inc} = 0 degree						
1	0.0575	-1.3	-1.71	-1.13	—	—
2	0.0587	0.8	0.24	0.82	—	—
3	0.0583	0.1	-0.60	-0.02	—	—
4	0.0585	0.4	-0.26	0.32	—	—
---------- line of symmetry ----------						
rms value	—	0.791	—	0.716	—	—
(r) Z = 600 + j0 ohms; $\beta h = \pi/2$; ϕ_{inc} = -40 degrees						
1	0.0589	4.65	-4.8	—	-115.4	0.3
2	0.0558	-0.85	-120.2	—	-113.9	1.8
3	0.0551	-2.1	-234.1	—	-114.6	1.1
4	0.0561	0.32	-348.7	—	-116.3	-0.6
5	0.0574	1.99	-465.0	—	-117.2	1.5
6	0.0574	1.99	-582.2	—	-116.4	-0.7
7	0.0558	-0.85	-698.6	—	-113.4	2.3
8	0.0538	-4.41	-812.0	—	—	—
rms value	—	2.62	—	—	—	1.36

Security Classification

DOCUMENT CONTROL DATA - R & D

(Security classification of title, body of abstract and indexing annotation must be entered when the overall report is classified)

1 ORIGINATING ACTIVITY (Corporate author)	2a REPORT SECURITY CLASSIFICATION
Naval Research Laboratory Washington, D.C. 20390	Unclassified
	2b. GROUP

3 REPORT TITLE

THE SCATTERING OF A PLANE ELECTROMAGNETIC WAVE BY A LINEAR ARRAY OF CENTER-LOADED CYLINDERS

4 DESCRIPTIVE NOTES (Type of report and inclusive dates)

A final report on one aspect of the problem.

5 AUTHOR(S) (First name, middle initial, last name)

O. D. Sledge

6 REPORT DATE	7a. TOTAL NO. OF PAGES	7b. NO. OF REFS
June 6, 1968	44	5

8a. CONTRACT OR GRANT NO.	9a. ORIGINATOR'S REPORT NUMBER(S)
NRL Problem R02-44 b. PROJECT NO. ARPA Order 820 c. d.	NRL Report 6681 9b. OTHER REPORT NO(S) (Any other numbers that may be assigned this report)

10. DISTRIBUTION STATEMENT

This document has been approved for public release and sale; its distribution is unlimited

11. SUPPLEMENTARY NOTES	12. SPONSORING MILITARY ACTIVITY
	Advanced Research Projects Agency, Washington, D.C. 20301

13. ABSTRACT

The scattering properties of a linear array of parallel, center-loaded, cylindrical elements have been investigated with the ultimate objective of obtaining information about the character of the array from its scattered field. To this end, a set of integral equations for the currents induced in the linear array illuminated by an incident plane wave were derived from the equations of Maxwell and the boundary conditions at the surface of the array. Using a zero-order approximation to the form of the axial distribution of the induced currents in the array, a pair of complex current coefficients were calculated numerically for each element of the array using a technique incorporating the set of integral equations. The approximation technique gives reasonable accuracy in the calculation of the *H*-plane, far-zone, scattered field from the induced currents, provided the electrical half-length of the elements of the array is less than $5\pi/4$ radians.

The scattered field of an eight-element array was calculated for various conditions of impedance loading and illumination of the array.

A significant result of this investigation was the discovery that the *H*-plane scattered field of a linear array of cylindrical elements illuminated by a plane electromagnetic wave consists of two factors: a reflection factor and an

(over)

14 KEY WORDS	LINK A		LINK B		LINK C	
	ROLE	WT	ROLE	WT	ROLE	WT
Antenna array						
// plane						
Scattering properties of antenna arrays						
Reflection factor						
Interference factor						
Interelement spacing						
Plane of polarization						
Resonant frequency						
Transducer						
Load impedance						

interference factor. The interference factor is simply the complex array factor of the array when excited with a uniform amplitude and an element-to-element phase progression of $2\pi(d/\lambda)\ \sin\ \phi_{inc}$ radians, where (d/λ) is the interelement spacing of the array in wavelengths and ϕ_{inc} is the angle of incidence of the illumination. The reflection factor turns out to be the //-plane scattered field in the reflected direction where the interference factor becomes unity.

From the interference factor we determined the positions of the grating lobes and the minima of the //-plane scattering pattern of the array for various plane-wave illuminations.

It was found that the plane of polarization of an array, the number of elements, the interelement spacing, and, possibly, the resonant frequency of the elements can be determined from the //-plane scattering characteristics of the passive linear array of cylindrical elements.